AIR FORCE INSTITUTE OF TECHNOLOGY

AIR UNIVERSITY
UNITED STATES AIR FORCE

GASDYNAMIC EVALUATION OF
CHOKING CASCADE TURNS

THESIS

Dennis R. Perez
Capt, USAF

AFIT/GAE/AA/84D-21

SCHOOL OF ENGINEERING

WRIGHT-PATTERSON AIR FORCE BASE, OHIO

AFIT/GAE/AA/84D-21

GASDYNAMIC EVALUATION OF CHOKING CASCADE TURNS

THESIS

Dennis R. Perez
Capt, USAF

AFIT/GAE/AA/84D-21

Approved for public release; distribution unlimited

AFIT/GAE/AA/84D-21

GASDYNAMIC EVALUATION OF CHOKING CASCADE TURNS

THESIS

Presented to the Faulty to the School of Engineering
of the Air Force Institute of Technology
Air University
in Partial Fulfillment of the
Requirements for the Degree of
Master of Science in Aeronautical Engineering

Dennis R Perez
Capt USAF

December 1984

Preface

Aerospace vechile designs are often volume limited, requiring extensive integration of components. One such component is the air intake systems which are needed for environmental, electrical, and propulsion devices. Typically these integrated designs result in peculiar internal ducting of compressible flows. For vechiles operating in the compressible fluid regions great care is required to preserve the total pressure. A research project was proposed by Mr. David B. Wilkinson, an aerospace engineer with the Ramjets Division of the Air Force Wright Aeronautical Laboratiory (AFWAL/PORA), to combine flow alignment, turning, and distortion control functions into a single cascade of aerodynamically-shaped guide vanes. Previously, Capt Jason Baird showed in a 1982 AFIT study the feasibility of different cascade designs. His study used the 43 inch water table for flow visualization. This work extends that effort to a gas dynamic evaluation of the proposed turn systems.

I want to thank Mr. Wilkinson for his ideas and assistance throughout my study. Also, I would like to thank Mr. Carl Shortt and Mr. Russell Murray of the AFIT Shops for their excellent work in the construction of the turning sections used in my study. I would like to thank Mr. Nicholas Yardich, Mr. Leroy Cannon, and Mr. Harley Linville for their asistance in setting up the air supply.

I would like to thank Dr. W. C. Elrod, Dr. M.E. Franke, and Capt W. Cox for their guidance during my study. Most of all, I thank my wife, Julie, and the kids; Elizabeth, Jeffrey, Nicholas and Lara, for all their support they gave me during my thesis work.

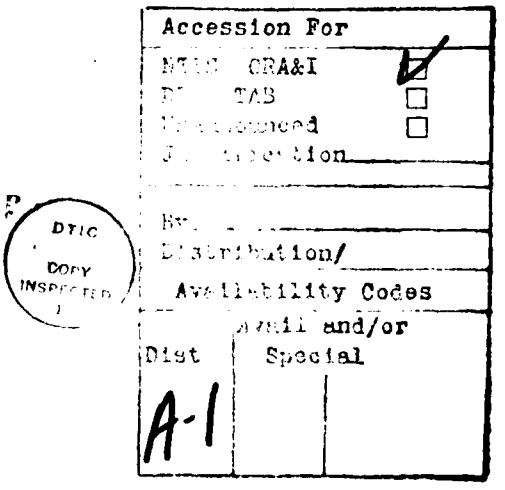

Table of Contents

List of Figures

List of Tables

Abstract

Uses for ram air in airborn vechiles are increasing along with the need for sophisticated ducting of the compressed air. Inlets operating supercritically, a normal shock in the subsonic diffuser, use an aerodynamic grid to control the normal shock posistion to a region of low total pressure losses. Turning of the flow requires long radius curves to maintain the total pressure. This study combines the internal shock posistioning and flow turning into a flow choking cascade turn with a short radius. Several sets of 90 degree turning sections, for turning compressed air, were selected, designed, and tested gas dynamically. Two of the turn sections were totally subsonic and only turned the air flow. Two other sections turned and choked the flow during supercritical inlet operation. These flow controllers perform the same function as an aerodynamic grid and flow turning vanes used in current internal compressible airflow designs . These tests correlated the suitability of using a water table versus a gasdynamic apparatus for determining the flow control capabilities and pressure recovery of the cascades. The subsonic only turning section gave the best pressure recovery and total pressure distribution along the turning axis, but allowed the supercritical internal shock to move towards large shock/boundary layer interaction. The

two shock positioning cascades provided good internal shock control with only slightly lower pressure recovery. Further investigation is needed of the effects of back pressure fluctuations on the flow dynamics.

I. Introduction

Purpose

Compressible flow turning is becoming more important in aerospace configurations. Use of externally scooped ram air in aircraft and missile systems allows designers more flexible configurations which could determine whether a system is feasible or not. Such systems could include: using ram air for an auxiliary power unit, inlets for propulsion, probes for arming warheads, ducts for cooling or heating systems, and many other uses. Some of the designs require ducting of the incoming flow in a different direction from the inlet axis. Also some designs incorportate an aerogrid (or venturi array) which controls the inlet internal shock position for some inlet operating conditions (Ref 14). The current designs use large radius turns plus a grid to turn the flow and control the shock position. This research studies the combination of an abrupt vaned, or mitered turn of short radius with an aerodynamic grid, resulting in reduced weight and volume and improved pressure recovery compared to the current designs.

This study will focus on systems used in the supersonic flight regime. Most of the uses for this air flow is in the subsonic region, so accordingly, a system of inlet shocks compress the air and decelerate the air flow to a useable velocity. This study will not focus on the different external shock-compression configurations but on the

internal diffuser and turning which immediately follow the external portion of the inlet. Supercritical inlet operation yields the optimum for pressure recovery and stability of the inlet shock system (Ref 13), so this mode of operation will be investigated.

Background

In the late 1950's, The Marquardt Company studied means to obtain better pressure recovery of inlets operating within the wide envelope of supersonic missile applications. One of the concepts that evolved from their efforts was a venturi array, or aerodynamic grid which created enough flow resistance to keep the internal diffuser shock in the low total pressure loss region of an inlet operating supercritically. This aerogrid concept is still being adapted to present day ramjet inlet systems (Ref 5). Mr. D Wilkinson of the Ramjet Applications Branch of the Aero Propulsion Laboratory (AFWAL/PORA) combined a turning requirement and the aerogrid into a single choking cascade turn. Captin Baird in 1982 performed a water table study which investigated the flow choking and flow turning capabilities of a choking cascade turn (Ref 2).

Objectives of Study

The objectives of this study were to experimentally investigate internal diffuser shocks and to gasdynamically evaluate the flow patterns and pressure recovery of choking cascade turns. This study was to quantify the pressure

recovery of diffuser shock posistions relative to the diffuser throat and verify the need for controlling internal diffuser shocks. The primary objective of this study is to gasdynamically evaluate the various combinations of turning vanes with an aerodynamic grid, to see if air flow turning and internal inlet shock positioning functions can be combined into one cascade.

Scope of Study

The principles involved in inlet operation and efficient airflow turning were researched in depth to gain an understanding of the mechanics and dynamics of aerodynamic grid and turning vane operation. Intake and airflow modes of inlet operation were investigated for use in an aerospace system. A one dimensional analysis was preformed to size the test components. Four turning models and a reference aerogrid were then designed, built and gasdynamically tested with schlieren photographs taken of the internal diffuser and the flow choking cascade section to give a better understanding of the mechanisms involved in both areas. Pressure measurements determine how well the turns were working from both a pressure recovery and a total pressure distribution standpoint.

II. Background Theory

In order to develop cascade designs and inlet diffuser test apparatus, it was necessary to consider how two dimensional inlets operate, note the problems with supercritical operation and how to control these problems, and finally investigate the dynamics of flow turning. The following sections provide background theory which give an understanding into compressible flow turning.

Two Dimensional Inlet Operation

Current intake designs proposed by the aerospace community use two-dimensional inlets for supersonic compression of ram air. The two-dimensional designs have proven easier to integrate into a vehicle package as compared to their axisymetric counterparts since they do not interfere with other components like: radar antennas, warheads, electronic bays, cockpits and fuel tanks. Nine different modes of inlet operation can be encountered (see Figure 1). The "on design Mach number" combined with critical back pressure yields the best pressure recovery with a minimum of external drag. Unfortunatly aerospace vehicles encounter a variety of Mach numbers throughout any particular mission and the back pressure can vary depending on the particular ram air usage. Subcritical and critical operation are usually avoided because these modes are unstable. In these cases, high back pressures allow subsonic feedback to interact with

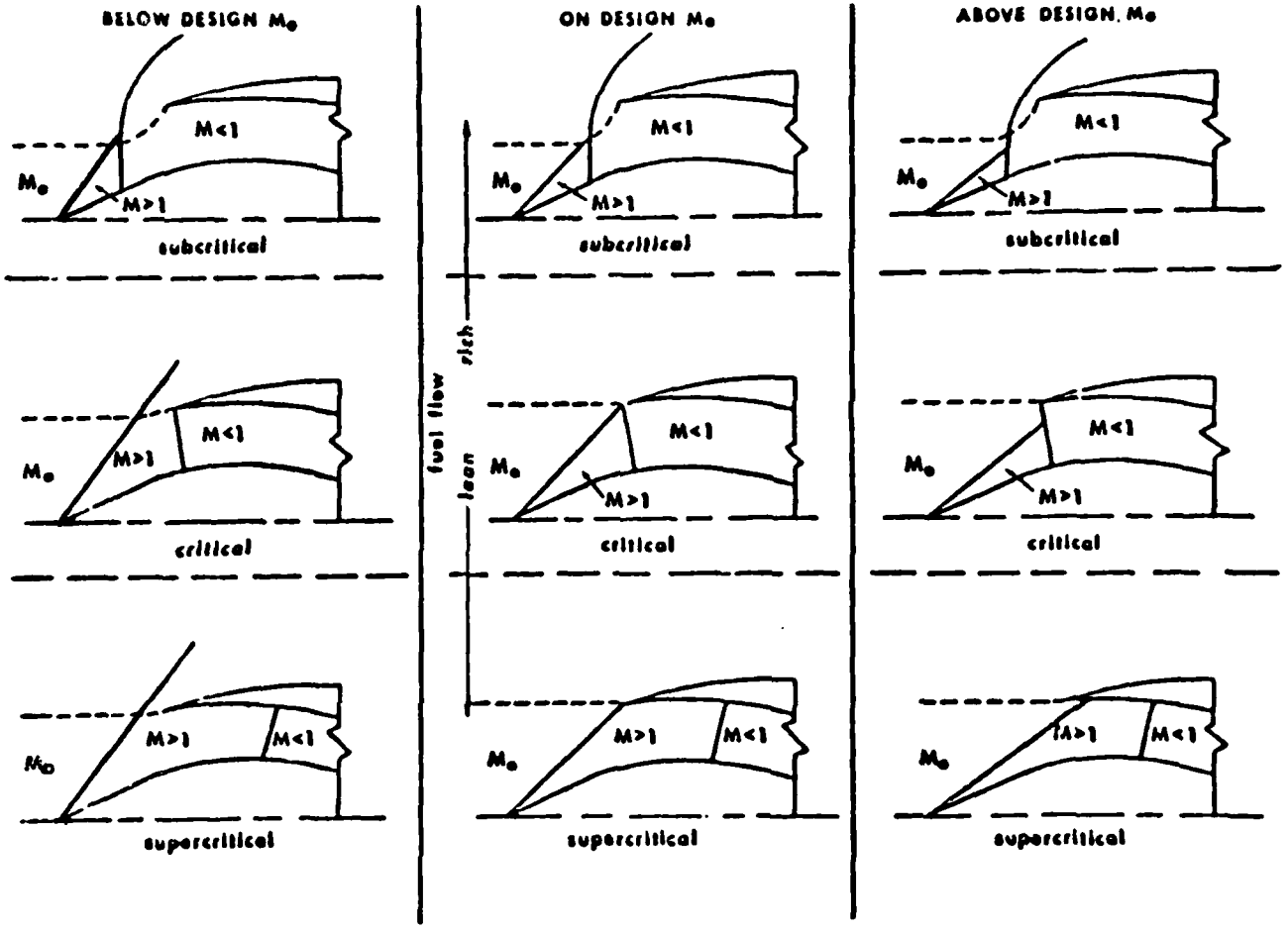

Fig 1 Supersonic Inlet Flow and Shock-Wave Patterns (Ref 12)

the external shocks, thus creating inlet buzz. Critical operation is actually just a break point between subcritical and supercritical modes of operation and trying to design just at this point could create instability problems, because a reduction in velocity or a increase in back pressure could drive the inlet to subcritical operation with its associated problems. Reference 6 provides more details on inlet operation.

Supercritical Inlet Operation

Supercritical inlet operation is when the inlet diffuser throat is supersonic and the flow in the internal diffuser is both supersonic and subsonic. As long as the internal normal shock remains near the throat the total pressure losses across the shock will remain low. When the back pressure is decreased, the shock moves down the internal diffuser creating a stronger shock which decreases the total pressure downstream and also interacts more with the diffuser's boundary layer. Reference 3 describes the shock-boundary layer interaction in detail for this internal two dimensional diffuser. Figure 2 shows how the stronger shocks create more uneven flow across the channel. This shock-boundary layer interaction creates a nonhomogenous flow which when enterng the component using the flow could reduce its efficiency. If the back pressure were low enough supersonic flow could enter the component, which is designed to use subsonic flow.

In order to control the amount of supercritical

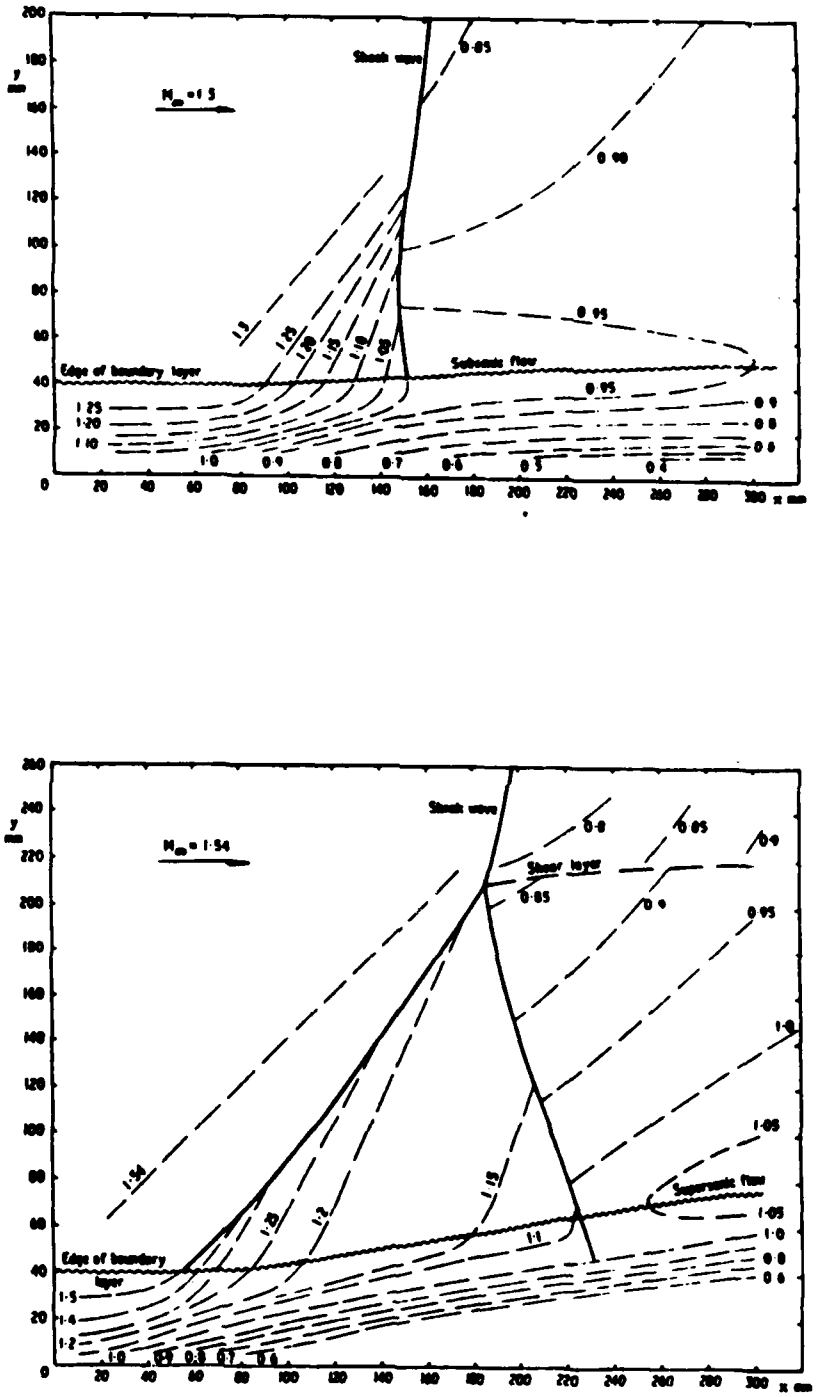

Fig 2 Flow Structure of Normal Shock-wave Boundary-layer Interaction

(Ref 3)

operation one could regulate the fuel control in a propulsive component or use an aerodynamic grid. Control by fuel flow does not appear promising due to the detailed knowledge required of how the inlet is operating at a variety of altitudes, mach numbers, and back pressures. With today's electronic processing cababilities this method of control could be done, but puts another burden in the electronic suite. The aerodynamic grid, invented in the late 1950's (Ref 15), positions a venturi array aft of the internal diffuser and forward of the combustor in a ramjet engine. During critical inlet operation, flow through the venturis is subsonic throughout. As the back pressure is decreased, the flow in the venturis eventually chokes leaving the internal diffuser shock at a low supercritical region, a position with low shock total pressure losses. As the back pressure further decreases, shocks now form in the venturis while the shock in the main internal diffuser remains stationary. This prevents increased shock-boundary layer interaction which decreaes pressure recovery and distorts the velocity profile across the diffuser (Ref 15: 3-5). Another added benefit of the aerodynamic grid is better air flow profile caused by having small channels controlling the flow over the entire cross section (Ref 14).

Combining the aerogrid and diffuser for a diffusing grid configuration delivers poorer performance than a fully developed boundary layer diffuser and grid configuration (Ref 4:15-19). When the flow is only partially diffused, the

boundary layer creates a velocity gradient which causes the side diffusing channels to operate with a nonuniform velocity distribution , see Figure 3a. A fully developed boundary layer in the diffuser provides enough energy transfer in the entire diffuser width for a more even velocity distribution which the aerogrid can control, (see Figure 3b). The result is that the flow must be first diffused in a long diffuser before it can be passed through an aerogrid (Ref 4:14-19).

Flow Turning

In some applications, the inlet is not on the same axis as the component using the flow. It is desirable to turn the flow with a good pressure recovery, and the turning may be done by a diffuser duct of either short or long radius. A long radius turn has better pressure recovery, but necessitates a longer flow passage, and therefore more wall friction losses than in a short radius turn. Also, the longer inlet would be heavier, and it might obstruct critical components. However, a properly designed set of guide vanes in a miter turn can reduce the energy losses, and make the performance of the turn competitive with the long radius turn, (see Figure 4).

Fluid flow around an unvaned miter turn is accompanied by a change in the cross-sectional velocity profile of the fluid, by a spiralling motion and by turbulence in and after the bend (Ref 11: 138). There are two main flow separation zones in a miter turn with smooth walls. One is next to the

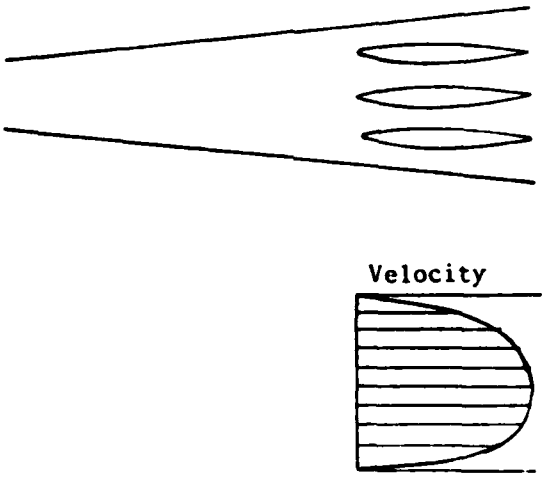

A Diffusing Grid

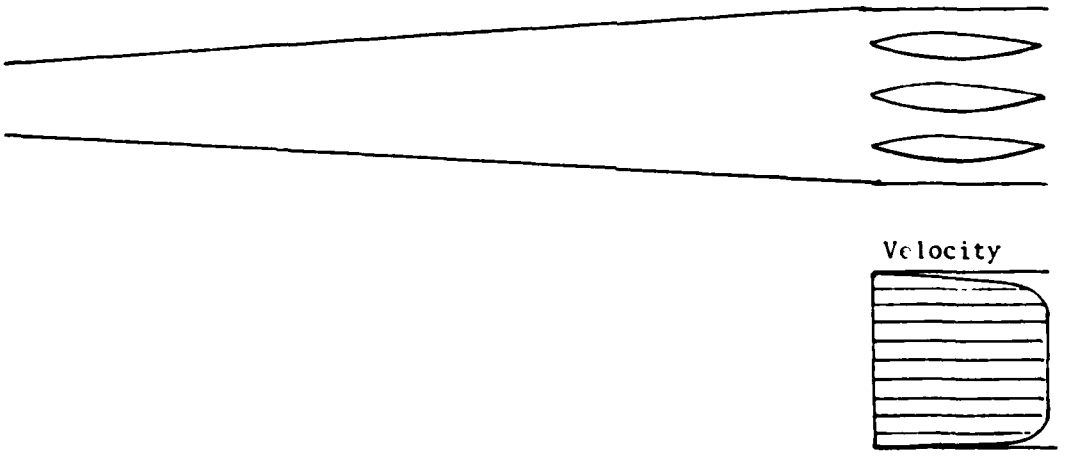

B Diffuser and Grid

Fig 3 Diffusing Grid vs Diffuser and Grid

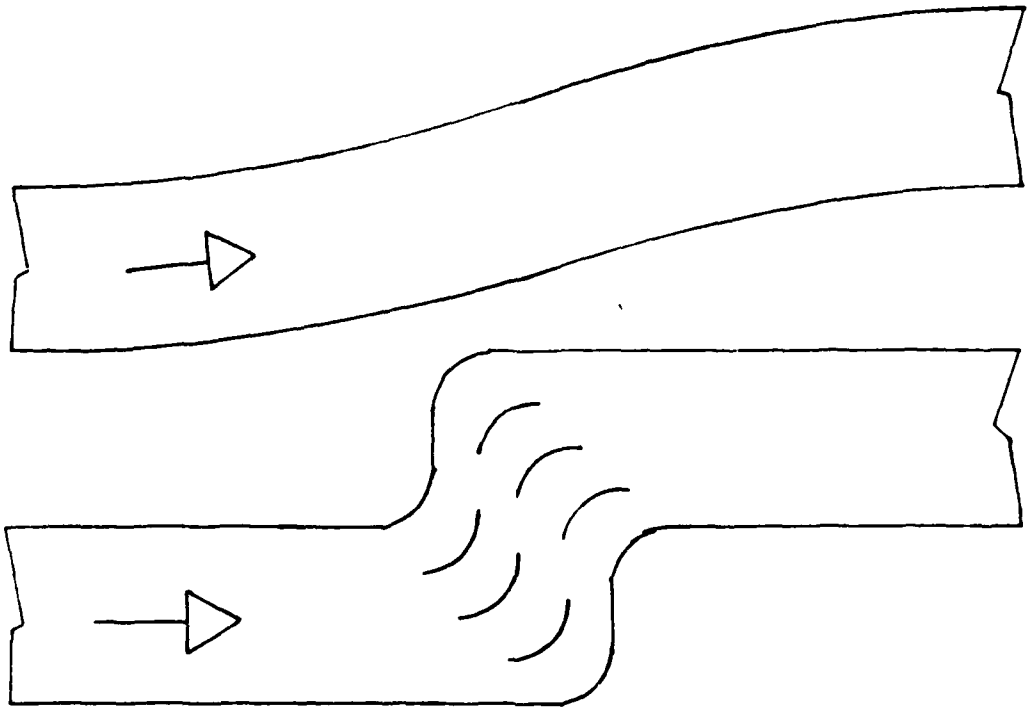

Fig 4 Long Radius Turn vs Cascades

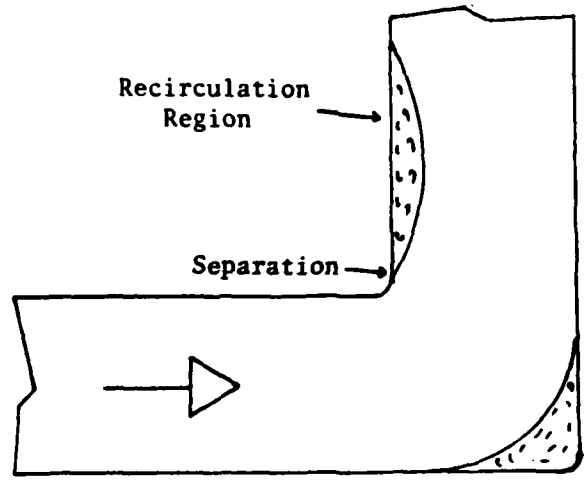

Fig 5 Unvaned Turn with Turbulent Zones

outside wall, and the other is on the inside wall immediately after the turn, (see Figure 5) (Ref 11: 138). Centrifugal force, on the fluid particles as they go around the turn, causes an increase in pressure that forces their velocity to almost zero near the outer wall. The flow separates, and eddys result on the outer corner. Fluid inertia and low fluid velocity, due to shear forces near the inner wall of the turn, cause flow separation from the inner wall immediately after the turn (Ref 11: 138). The pressure gradient across a turn also causes secondary flow, or a twin eddy in the fluid, (see Figure 6a). The static pressure is low near the inner wall, it increases with radial distance across the bend, and then it rapidly drops off as the separated region near the outside wall is approached, (see Figure 6b). This reduction in pressure causes an outward motion of the fluid, which turns into a double vortex through the turn. All this extra fluid motion adds to the friction losses, and creates more downstream turbulence in the fluid (Ref 11: 147).

The introduction of guide vanes, or splitters, into the turn divides the turn channel into passages with larger radius and aspect ratios, and reduces the pressure losses. The radius ratio of the passage is its radius of curvature divided by its hydraulic diameter (the hydraulic diameter is four times the cross-sectional area divided by the wetted perimeter). The aspect ratio (for rectangular passages) is the width of the short side of a passage, divided by the

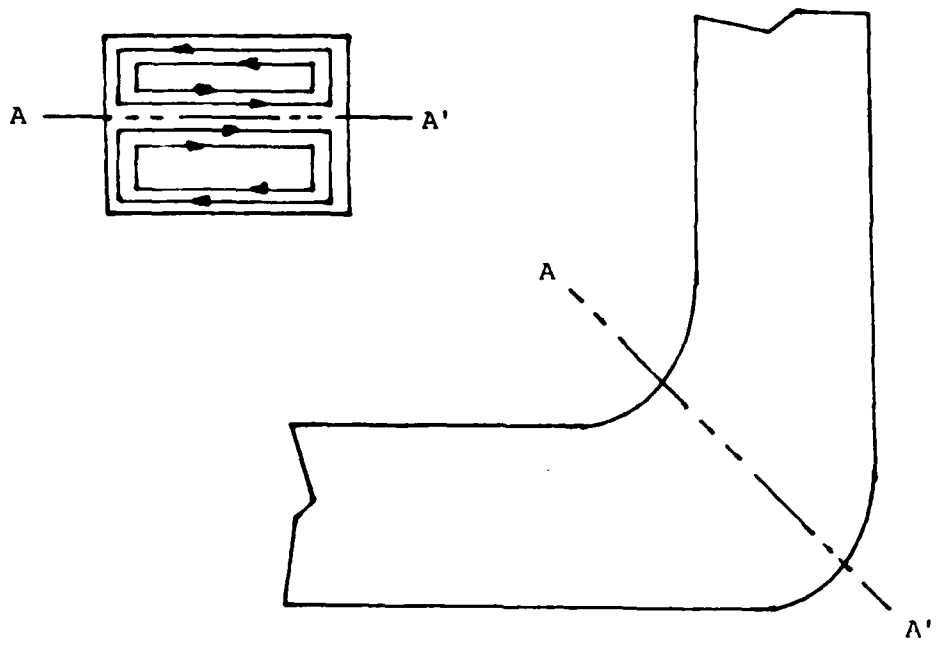

A Twin Eddy in Turn

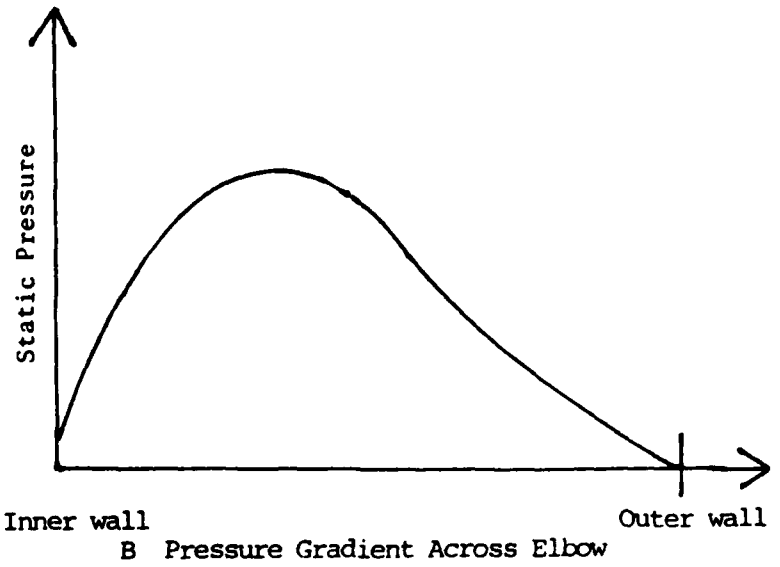

B Pressure Gradient Across Elbow

Fig 6 Miter Turn (Ref 11)

length of its long side. The flow resistance of a passage is affected inversely by these two ratios, as might be expected from the above explanation of flow losses. Insertion of guide vanes into a miter turn changes it from a short radius turn to a number of long radius turns with larger radius and aspect ratios, when the radius of curvature of each vane is the same as the radius of curvature of the inner wall of the turn (Ref 7: 373).

Designing the guide vanes with airfoil cross-sections introduces desirable effects. Such an aerodynamic cascade combines the good radius and aspect ratios of guide vanes with stream deflection toward the inner wall of the turn by downwash from the airfoils. When the proper vane angle-of-attack is selected, this deflection prevents flow separation from the inner wall of the turn. A well-designed cascade reduces elbow flow resistance and improves the velocity distribution after the elbow.

For a uniform velocity profile after the turn, or uniform total pressure profile, an optimum gap-to-chord ratio is 0.3 to 0.4 for air flow (Ref 16: 4). The gap-to-chord ratio is the ratio of height of the smallest part of the flow passage between two adjacent vanes, to the vane chord length. As the gap-to-chord ratio is reduced, the radius and aspect ratios are increased and the pressure drop will decrease, until the wall friction losses increase enough to offset the drop (Ref 7: 373).

III. Design of Test Apparatus

This section describes how the shapes of the different components used in this study were selected. Only the components in the test setup that required special internal aerodynamic consideration are discussed. Equations for sizing components are described in Appendix A.

Internal Diffuser

A convergent-divergent nozzle was used to simulate the throat and subsonic diffuser of a supersonic inlet. This application is acceptable considering that in supercritical inlet operation, flow at the throat is sonic or supersonic and the diverging section accelerates the flow, then a normal shock converts the flow so that the remaining diverging section is a subsonic diffuser. When an aerogrid is used with this diffuser, it resembles another sonic region or a channel with two throats as described in Ref 10: 45. East in Ref 3 used a simular set up to get a simular effect.

The nozzle entrance region is designed for best pressure recovery as prescribed in Ref 9. Mulenburg showed in Ref 9 that straight 45 degree entrance ramps combined with an elliptical throat section gave good pressure recovery results. The elliptical throat section was replaced by a circular arc throat section for ease in construction in this study. In Ref 9 the circular arc

throat section worked as well as the elliptical throat section when the circular arc radius of curvature was two times the throat width.

The diverging section selected is not symmetric. This was chosen because in some applications one side could be an exterior wall which might be straight. So, all of the area change is done by one wall. An expansion angle of six degrees was chosen small enough to prevent adverse pressure gradient separation and large enough to prevent the boundary layer from interfering with the internal shocks (Ref 12). The resulting internal diffuser shape which combines the above considerations is shown in Figure 7.

Turn Section

Applications for internal turns of compressed air can direct the flow anywhere from 45 to 120 degrees from the inlet axis. This being an academic study, a 90 degree turn was selected because it was large enough to give the turning problems that might be encountered by actual applications. The turning section intake and exhaust dimensions allowed for dimensional compatibility with the diffuser exit and provided no diffusion. Lengths for the input and output sides were kept as short as possible, but still allowed for ease in hardware mating. Vane and blade leading edges were located on a 45 degree diagonal on the 90 degree mitered turn.

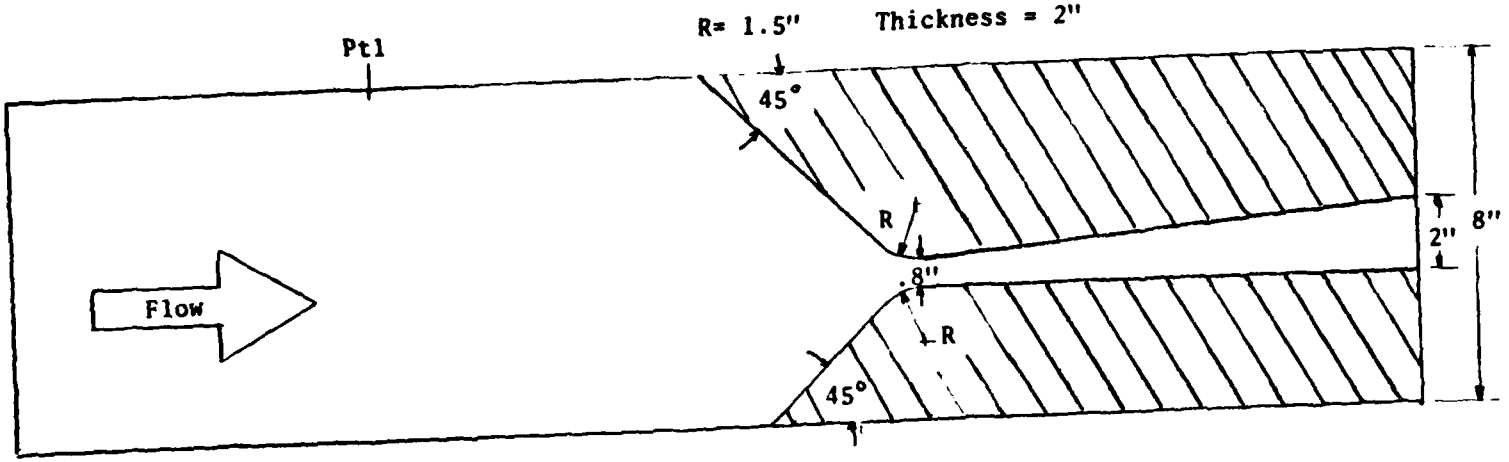

Fig 7 Test Section - Diffuser

Vane Design

This design allows for a subsonic controlled turn. The turning quality of this vaned turn is described in Ref 13. This design resembles the NASA transonic wind tunnel design which uses closely spaced vanes on the inner turn and gradually increases the spacing to the outer turn. This controls the flow by placing more channels on the inside of the turn where separation is most likely to occur. The vanes are thin 90 degree circular arcs, but are thick enough for structural rigidity. For an unvaned turn the middle vanes can be removed. See Figure 8 for a cross-sectional view and the turn setup.

Blade Design

Design criteria for good blade designs were given by Baird (Ref 2). The design criteria are: smooth wall curvatures, small trailing edge angle, large radius ratios, and medium amounts of blockage. Using the above design criteria, Baird's designs number 3 and number 5 were adapted for gasdynamic evaluation, see Figure 9. In conformance with these criteria, the following blade designs were selected for this investigation.

Blade Design 1. This design has sharp leading and trailing edges to provide very gradual area changes to the flow entering and leaving the turn. The flow chokes at 50% of the chord. See Figure 10 for a cross-sectional view and the turn setup.

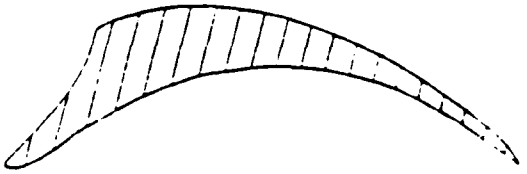

Design 1

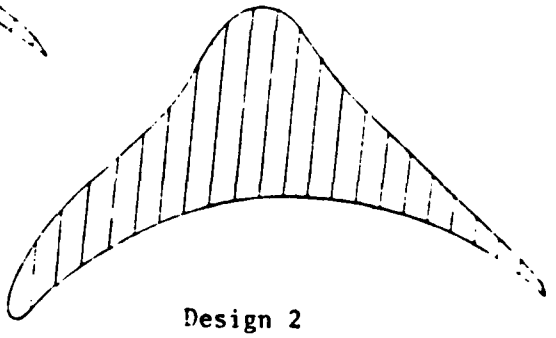

Design 2

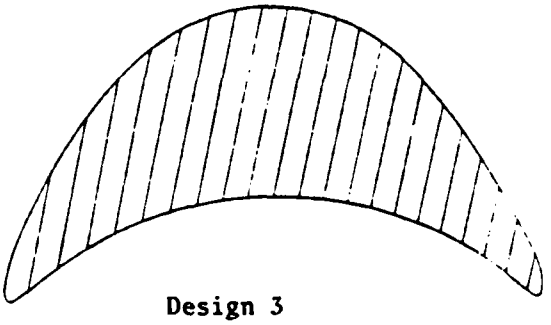

Design 3

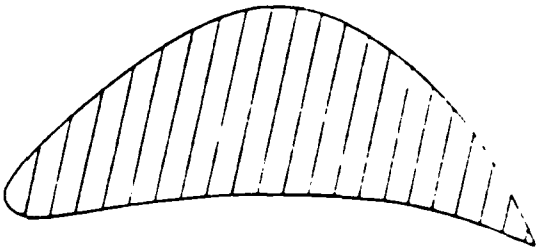

Design 4

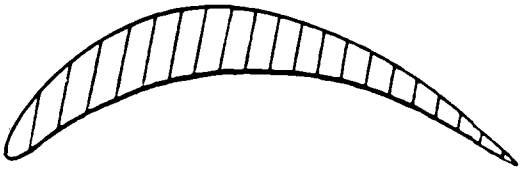

Design 5

Fig 9 Turning Blade Designs (Ref 2)

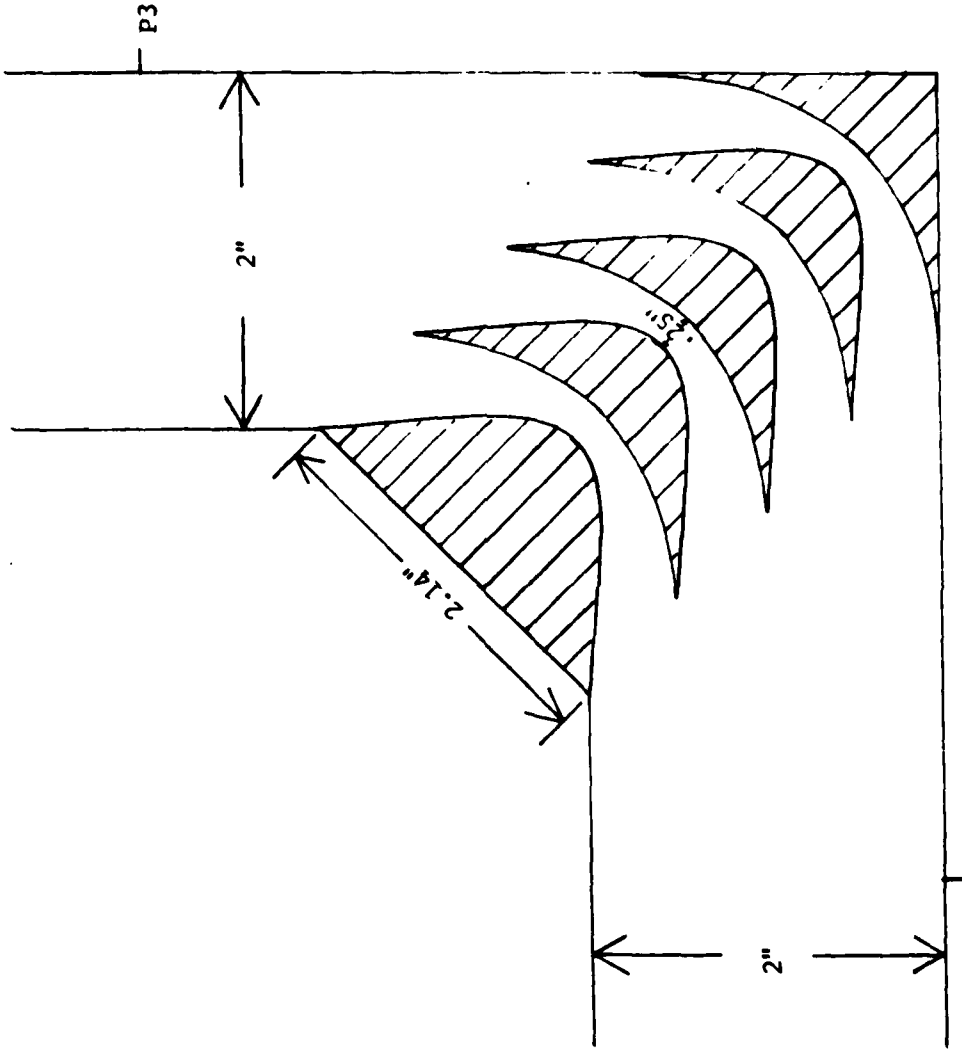

Fig 10 Turning Section with Blade Design 1

Blade Design 2. This design has a rounded leading edge and a small trailing edge angle. The minimum area occurs at 30% of the chord. Flow is choked early and the divergent channel is longer for better flow control in the diffusion process. See Figure 11 for the cross-section and turn setup.

Blade Design 3. This design is subsonic like the vane design. The flow turns early in the channel and exits with a small diffusion angle. The leading edge is semisharp to provide some tolerance to flow variations in the duct. The chord was reduced to 1.75 inches. This was done because the inner turn intrusion is the critical dimension in the design. See Figure 12 for cross-section and turn setup.

Aerodynamic Grid

The aerodynamic grid, or aerogrid, used design criteria described in Ref 15. A three blade, four channel, grid was selected so the data could be related to the turning section data. The chord and blockage design criteria used in the choking cascade turns were simulated in the aerogrid. Figure 13 shows the aerogrid setup.

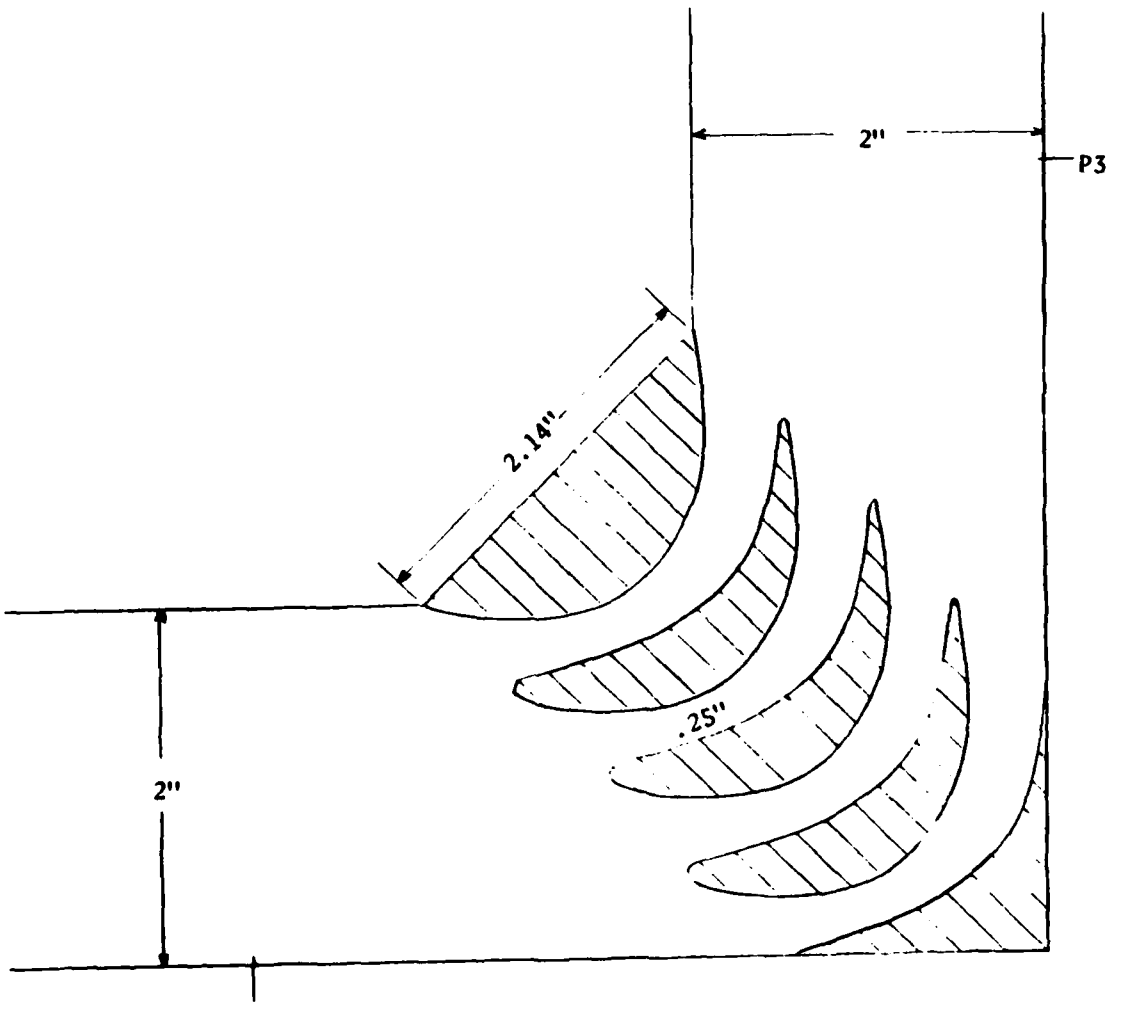

Fig 11 Turning Section with Blade Design 2

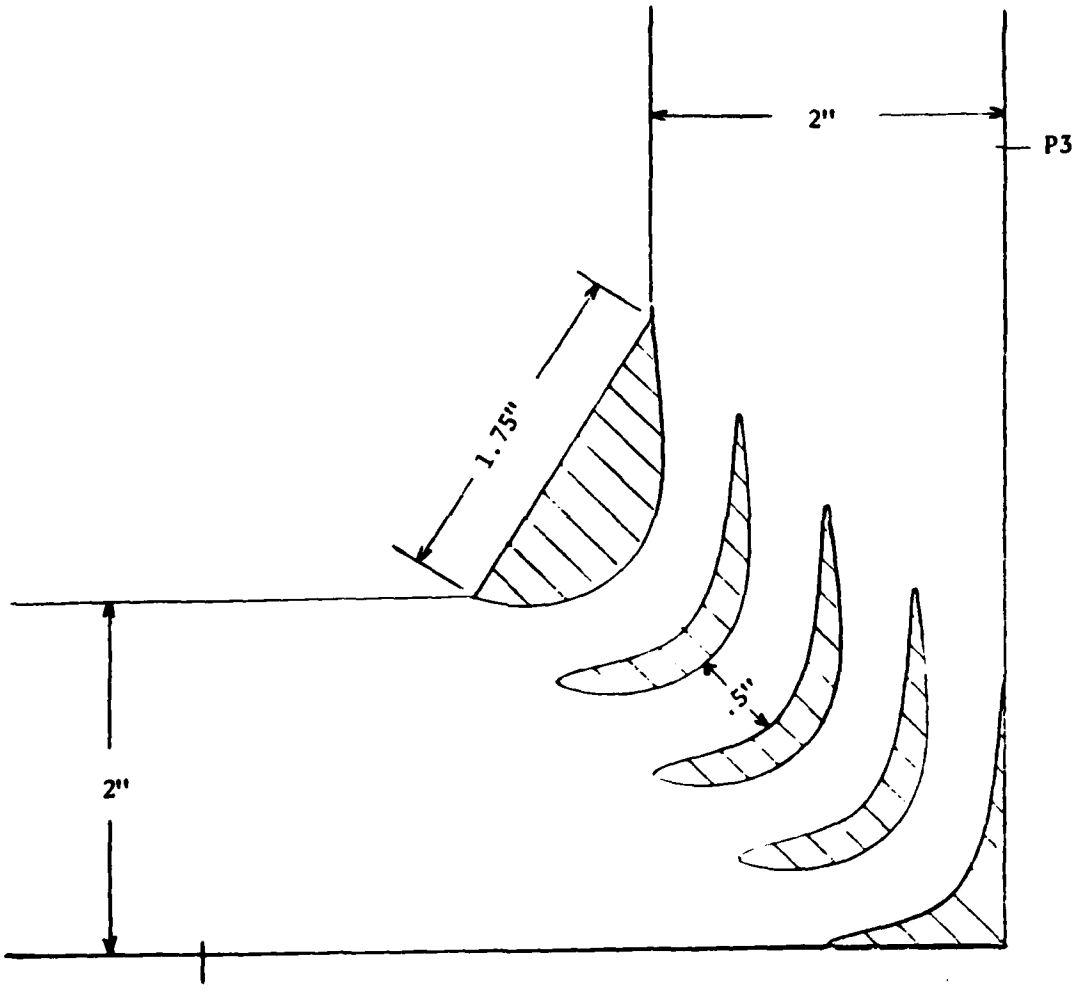

Fig 12 Turning Section with Blade Design 3

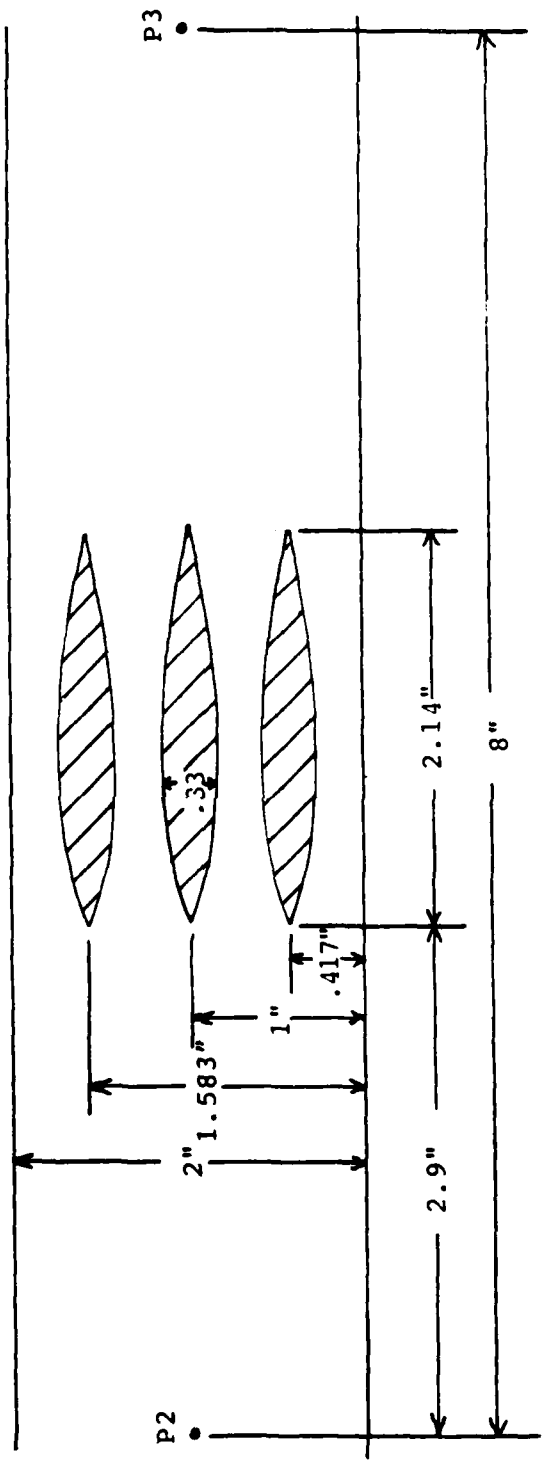

Fig 13 Aerogrid

IV. Experimental Equipment and Instrumentation

Experimental Equipment

Test apparatus used in this study used conventional shop materials and accessories. A description of the three major sections and their components are provided.

Air Supply. The AFIT 100 psi air supply was used for this investigation. The minimum size pipe encountered was three inches diamenter, which was located at the test station. Due to the moisture in the air and the amount of rust in the pipes, a cyclone separator was used to extract the large solid particles and water, and a 10 inch diameter paper filter was used to further clean the air flow.

Test Section. The test section was comprised of the throat and subsonic diffuser of a supersonic inlet, a short radius 90 degree turn with or without turning vanes or blades, and a valve to permit controlling the back pressure. A three inch diameter circular to a 2 by 8 inch rectangular section adapted the supply air to the test section. Optical windows, 6 by 20 by 0.75 inches were provided on one end of the throat and diffuser section, for viewing the air flow in the diffuser.

Turning Section and Cascades. Three different turning sections and four different cascade designs were constructed with an aluminum structure which sandwiched Plexiglas viewing sections containing aluminum blades or vanes. One turning section allowed for vanes made from three inch

diameter tubing to be positioned in the turn. This vaned section could be used with or without the middle vanes. This capability allowed for either a vaned turn or an unvaned turn. Another turning section allowed for either of two sets of shock positioning blades. Both blades were positioned so that their chord line was at a 45 degree angle to the incoming flow. The final turning section allowed for one set of blades to be put in with its chord at 63 degrees to the incoming flow.

Instrumentation

During the course of this investigation, two types of instrumentation were used, namely the schlieren optical system and a manometer pressure measuring system. A description of each of the two systems and its components is provided.

Schlieren System. The schlieren setup used in this study, shown in Figure 14, is a standard system with its principle of operation described in References 8 and 13. It consists of two concave mirrors, either a continuous light source or a spark lamp, a knife edge, and a camera assembly.

Mirrors. Two 7.5 inch diameter concave mirrors, with focal lenghts of 40 inches, were used in this system positioned as shown in Figure 14. They were mounted on optical stands with a vertical adjustment for proper positioning. A small mirror was inserted into the optical path to allow the use of a second light source, with the

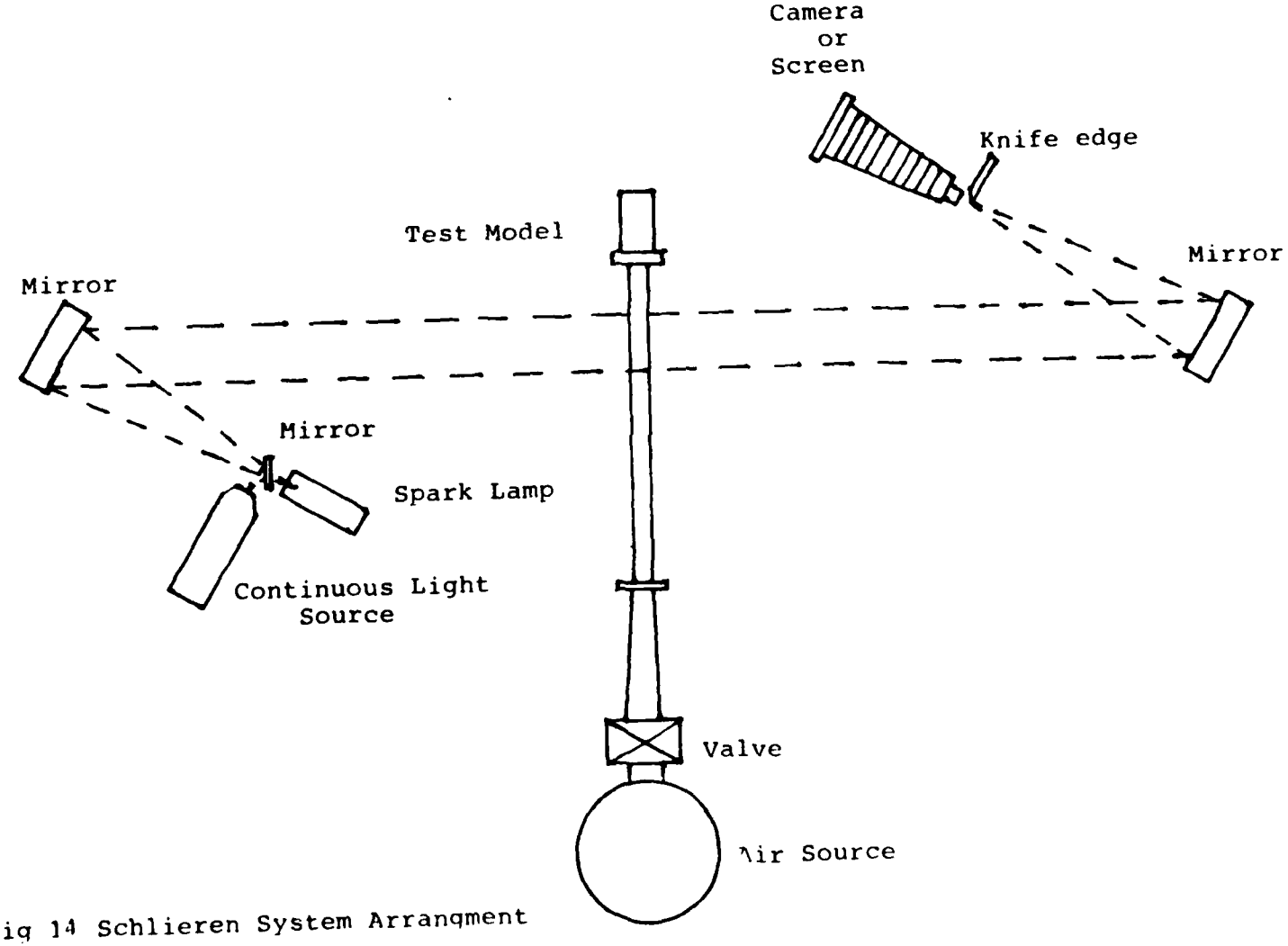

Fig 14 Schlieren System Arrangment

single set of concave mirrors.

Light sources. Two types of light sources were used: a continuous light source and a spark lamp. A continuous light source was required in aligning the system. This consisted of a high intensity lamp which was reflected off a small mirror onto one of the concave mirrors. This could also be used to observe an averaged flow pattern at real time with the use of a viewing screen on the camera assembly.

The second light source employed was a high intensity spark lamp with a flash duration of approximately a microsecond. Switching from the continuous light source to the spark lamp required only the removal of the small mirror from the optical path. The spark lamp provided the capability of "freezing" the flow due to the short, one microsecond, flash duration. The spark lamp is therefore invaluable in high speed photography for flow visualization.

Knife edge. The knife edge utilized in the system allowed for both vertical and horizontal positioning as well as the ability to be rotated to any angle. The knife edge was mounted on a stand in front of the camera assembly with the capability for fine adjustments.

Camera assembly. The camera assembly consisted of a camera bellows with a variable speed shutter and a polaroid camera back assembly. The polaroid camera could be replaced by a frosted glass screen for real time viewing purposes.

Manometer Pressure Measuring System. The air supply provided steady flow which allowed the use of a manometer pressure measuring system. A total pressure rake was made out of 0.035 inch diameter tubing with a 0.02 inch inside diameter. Twelve tubes were placed 1/6 inch apart. The end tubes were positioned 1/12 inch from the inside and outside walls of the flow channels as shown in Figure 15. A static port for measuring the stagnation chamber pressure was positioned in the test section as shown in Figure 7. Static ports for measuring the aerogrid and turning sections static pressure losses are shown in Figures 9 through 13. A pitot probe for measuring total pressure was positioned eight inches from the end of the turning section, (or the end of the diffuser for the nonturning tests). To record all 16 pressure ports, a photograph was taken of the manometer bank containing the pressures. Two manometer banks were used. Each manometer bank contained ten 40 inch mercury U-tube manometers. A standard barometer was used to record the atmospheric pressure. A polaroid land camera recorded the pressures on film.

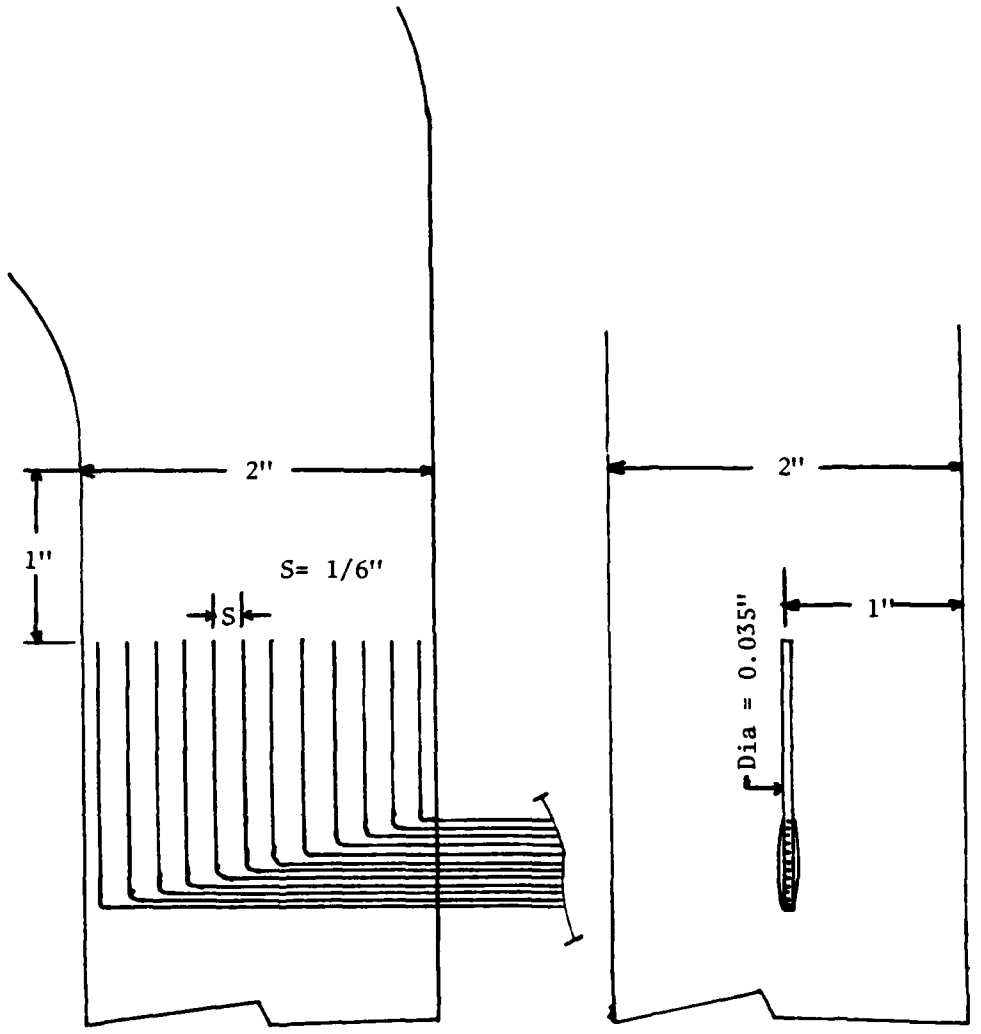

Fig 15 Pitot Rake

V. Results

This section presents the results obtained in the diffuser shock investigation and the total pressure recovery analysis. Internal diffuser shocks and shocks in the cascades visually showed the combined result of the shock positioning capabilities of the aerogrid and the choking cascade turns. Each configuration was quantitatively evaluated as to its pressure recovery capability. Results from different turn configurations are compared graphically.

Diffuser Shock Investigation

Diffuser shocks may be related to the amount of supercritical operation and it has been stated in many references (Ref 6,8, and 13) that operation too far into the supercritical region hurts the performances of the inlet. One reason is that the strong shocks dissipate more energy and another reason being the high shock-boundary layer interaction losses. Figure 16 is a composite of different schlieren photographs like those shown in Figures 17 through 20. At high back pressure ratios, Pt exit/Pt in, the shock-boundary layer interaction is small. As the pressure ratio decreases the shock-boundary layer interaction intensifies. In Figure 20 the shock-boundary layer is so intense that a multiple shock arises. This multiple shock is about equivalent to a single strong normal shock (Ref 13). Figure 21 shows how one dimensional, compressible flow

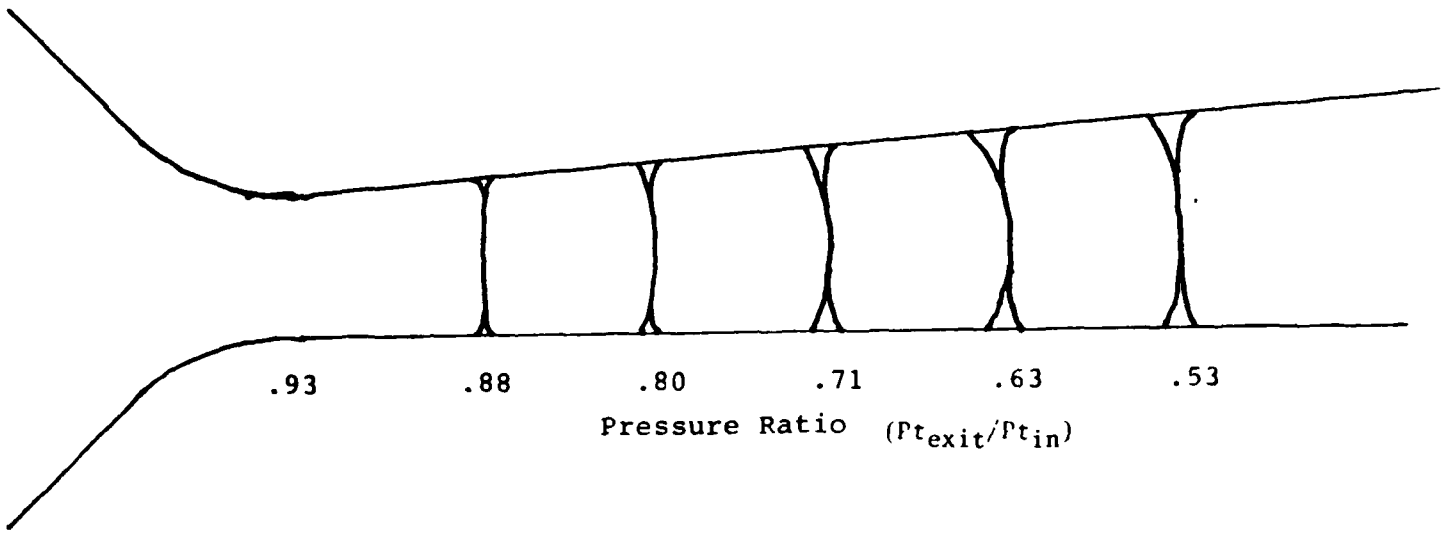

Fig 16 Diffuser Shocks at Different Pressure Ratios

Fig 17 Schlieren Photograph, Diffuser Shock, Vertical Knife Edge

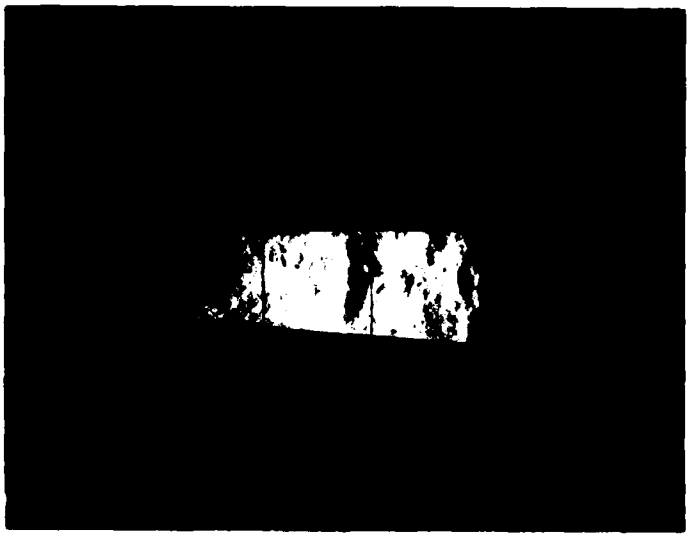

Fig 18 Schlieren Photograph, Diffuser Shock, Horizontal Knife Edge

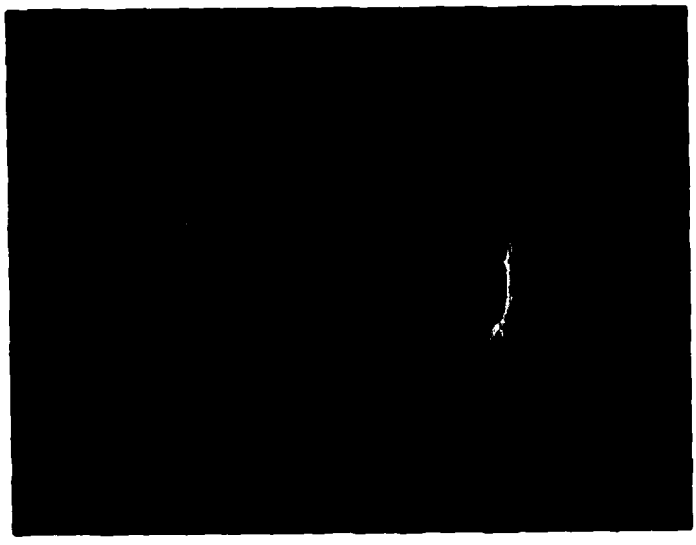

Fig 19 Schlieren Photograph, Diffuser Shock, Minimum Back Pressure

Fig 20 Schlieren Photograph, Multiple Diffuser Shocks

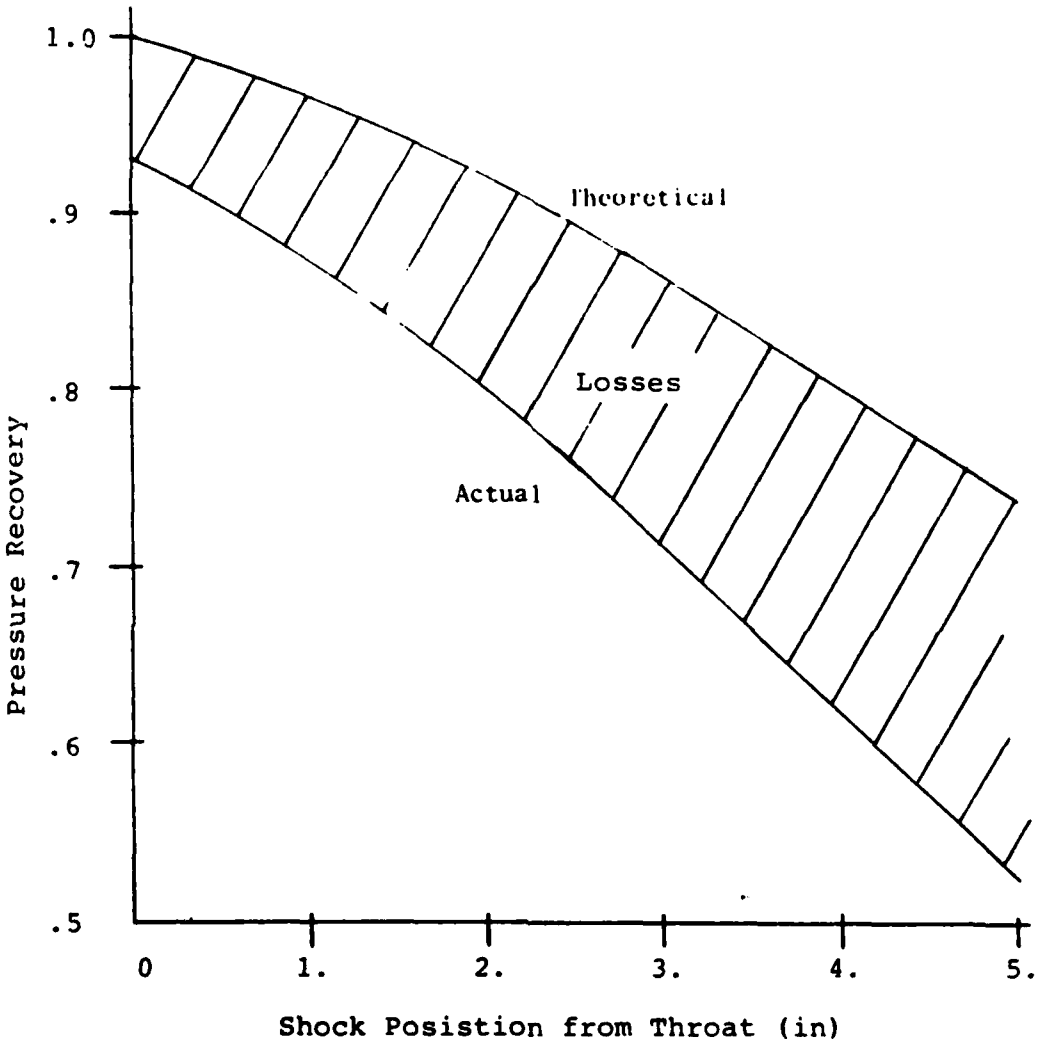

Fig 21 Pressure Recovery vs Shock Position

theory and the experimental results compare. The losses result from the shock-boundary layer interaction which causes momentum and friction losses. With the aerogrid or shock positioning cascades the diffuser shock stays within 2.5 inches from the throat and remains at 2.5 inches when the back pressure is further reduced. This internal shock positioning keeps the diffuser losses to an acceptable value. Figures 17 and 18 show the internal shock with low back pressure and a flow choking cascade in the flow. Figure 17 was obtained with a vertical knife edge in the schlieren system to highlight horizontal density gradients and Figure 18 uses a horizontal knife edge to highlight vertical density gradients. Figure 17 shows the shock clearly, whereas Figure 18 shows the boundary layer better.

Shocks in the aerogrid turns or straight sections result from the reduced back pressure creating a nozzle effect in the diverging section of the cascade channels. Figures 22 and 23 are schlieren photographs of the turn with blade design 1 installed. These photographs show the separation caused by the shocks interacting with the boundary layer and the large adverse pressure gradient created by the small radius turn in the diffusing flow passage. The inside channel has a more pronounced separation which extends almost across the entire channel, whereas the outside channel has less boundary layer separation across its channel, see Figure 23. Total pressure profiles described in the next section give further

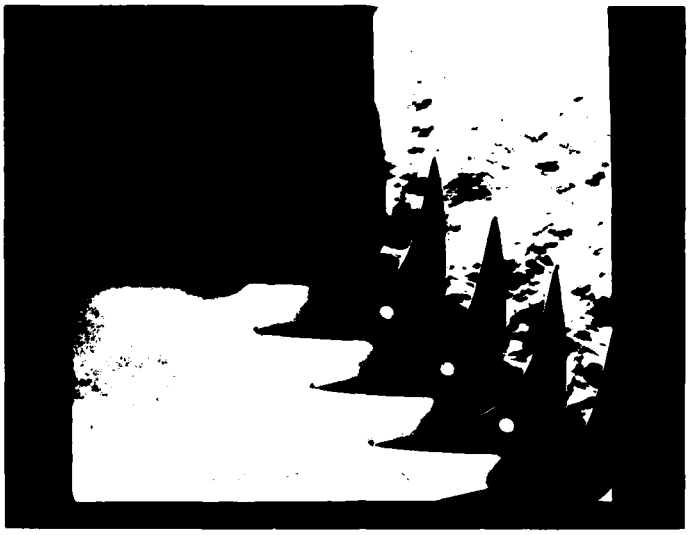

Fig 22 Schlieren Photograph, Blade Design 1, Vertical Knife Edge

Fig 23 Schlieren Photograph, Blade Design 1, Horizontal Knife Edge

evidence to this situation. Figures 24 and 25 are schlieren photographs of the turn with blade design 2 installed. This turn shows less separaton across each channel as compared to blade design 1. The oblique shock system converts the energy with less total pressure losses in blade design 2 than the shock and gross seperation in blade design 1. The large seperation in design 1 reaccelerates the flow and produces a second shock system that is not present in design 2. This could be attributed to the earlier choking and the longer diverging section that turns more gradually in the blade design 2 than in blade design 1.

Fig 24 Schlieren Photograph, Blade Design 2, Vertical Knife Edge

Fig 25 Schlieren Photograph, Blade Design 2, Horizontal Knife Edge

Pressure Recovery

Pressure recovery measurements provide a numerical basis for evaluating the performance of the diffuser-short radius turn system. Each configuration was tested with a minimum of three different total pressure ratios (Pt exit/Pt in); one at the critical pressure ratio (diffuser throat just sonic), another with minimum back pressure, and finally with a intermediate back pressure (typically with the internal shock two inches from the throat). Appendix B shows all the pressure recovery profiles taken for the systems.

To compare one configuration to another the values for critical inlet operation (shock at diffuser throat) are compared. Table I shows the different configurations at critical inlet operation with a mass flow of 1.076 lbm/sec. Pressure recovery values are the average total pressure ratios recorded by the pitot rake. All turning sections showed less pressure recovery when compared to the no turn data, which was two precentage points better than the vaned turn. The aerogrid and the blade design 2 recorded the same average pressure recovery, which shows that a flow choking cascade can have the same pressure recovery as an aerodynamic grid. The static pressure ratio, P3/P2, for the flow choking designs, were less than the subsonic only designs. The flow choking designs have more blockage which could caused the lower static pressure ratios. The delta pressure ratio column shows the amount of total pressure distortion on the curve. Figures 26 and 27 show the variation in pressure profiles on a single plot for subsonic only and flow choking only cascades. Both flow choking profiles show a dramatic pressure change in the inner channel, as compared to the other channels. Blade design 2's profile is not as radical as that for blade design 1. The unvaned turn shows a steady pressure gradient for the inside to the outside wall. The vaned turn showed only slight variations in pressure recovery across the turn.

Table I: Critical Operation

Mass Flow = 1.075 lbm/sec

	Ave PR	Delta PR	P3/P2
No Turn, No Aerogrid	.93	-	-
No turn, Aerogrid	.90	-	.96
Unvaned Turn	.90	.05	.99
Blade Design 1	.88	.11	.91
Blade Design 2	.90	.07	.97
Blade Design 3	.91	.05	.99
Vaned Turn	.91	.03	.99

PR = Pressure Recovery

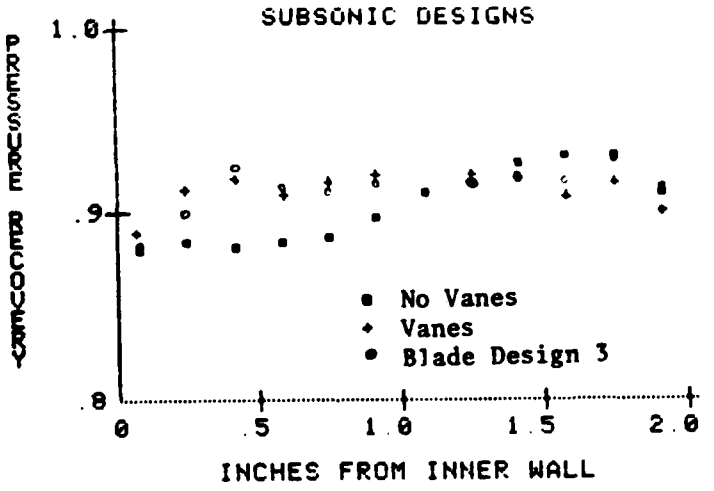

Fig 26 Pressure Recovery Distribution, Critical Operation Subsonic Designs

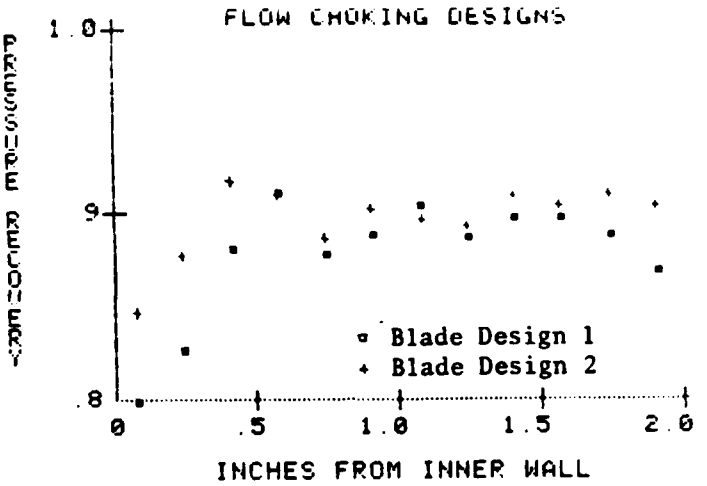

Fig 27 Pressure Recovery Distribution, Critical Operation Flow Choking Designs

A study was made to determine if variation of mass flow affected the results. Figure 28 shows that there is a tendency for the pressure recovery ratio to go down ith increased mass flow. This can be rationalized by the presence of more mass in the flow to cause more viscous losses. The resulting linear curve fit yields a linear equation having a 91.8% agreement if the data scatter at 1.075 lbm/sec is used and a 98.0% agreement if the data at 1.075 lbm/sec is averaged and then used. Figure 29 shows the pressure recovery profiles at different mass flows for blade design 2.

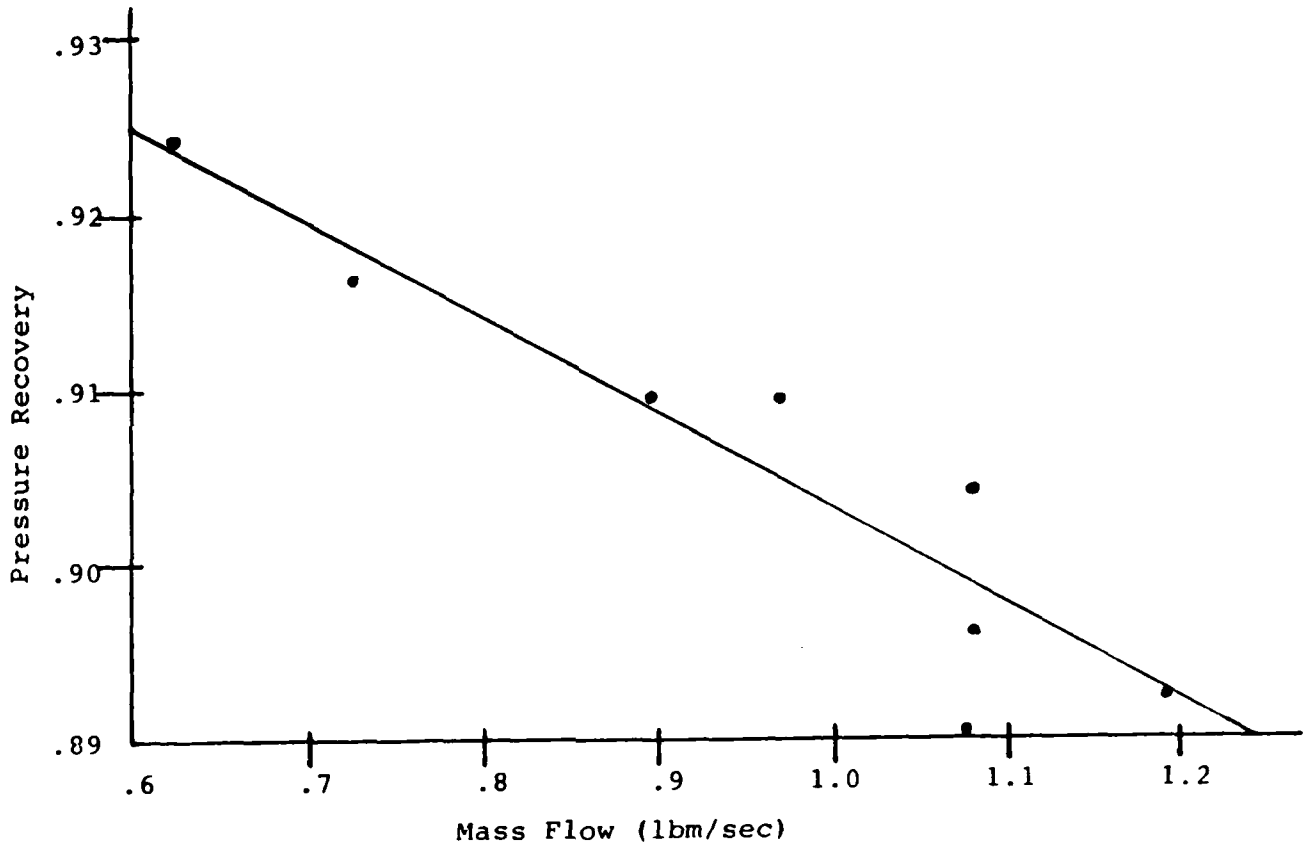

Fig 28 Pressure Recovery vs Mass Flow for Blade Design 2

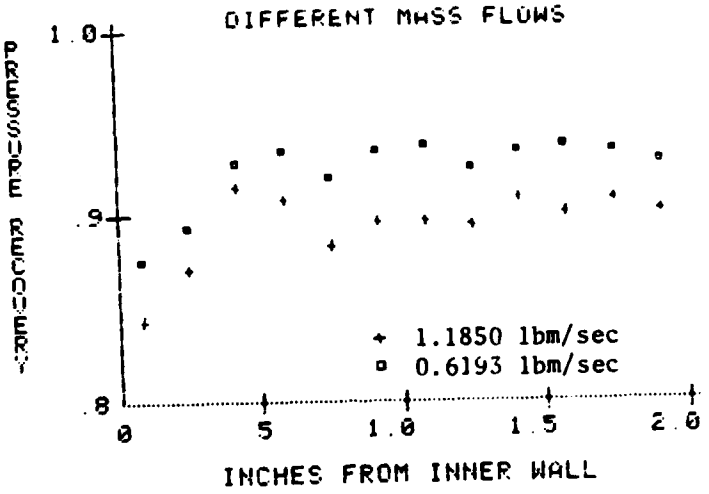

Fig 29 Pressure Recovery Distribution, Critical Operation, Different Mass Flows

Minimum back pressure data were taken to see how well the different configurations recovered the total pressure with a fixed physical back pressure. Table II shows the results. The unvaned turn exibited non periodic pressure flucations, which was caused by the separation region after the turn changing the nature of the blockage. The flow choking designs allowed for slightly better pressure recovery.

Table II: Minimum Back Pressure

Mass Flow = 1.075 lbm/sec

	Ave PR	Delta PR	P3/P2
No Turn, No Aerogrid	.60	-	-
Unvaned Turn	.60*	-	-
Blade Design 1	.66	.11	.69
Blade Design 2	.66	.08	.74
Blade Design 3	.65	.08	1.00
Vaned Turn	.64	.06	.99

PR = Pressure Recovery

* Erratic Pressure Readings

Other Observations

Back pressure fluctuations, caused by a loose gate on the back pressure valve, produced internal shock movements of 0.2 inches from a nominal position. This erratic behavior is attributed to the acoustic feedback of dynamic signals which are allowed to be transmitted in subsonic flows. All the configurations operating with subsonic flow from the internal diffuser to the back pressure valve experienced these flucations. When the flow choking cascades choked, the internal shock was steady, but when the choking cascades were unchoked (as in high back pressure situations) the internal diffuser shock moved like the other subsonic designs. A back pressure valve with a better fitting gate showed no erratic shock movement in any of the configurations.

VI. Conclusions and Recommendations

Conclusions

This study experimentally verified the need to control the intensity of the internal diffuser shock. Figure 21 showed the need to keep the shock position close to the throat in order to keep the shock and additional friction losses down.

This study verified gasdynamically that a flow-controlling cascade turn can be designed to accomplish the shock positioning function and to have a pressure recovery comparable to that of an aerodynamic grid. The shock positioning function of the choking cascade turns prevented the internal diffuser shock from moving into a diffuser region with more losses. Pressure recovery of the an airfoil shaped choking cascade blade compared equally with an aerogrid.

Recommendations

Based on this study, it is recommended that further research be extended to more diverse turn and choking designs. This new project would take the design philosophy used in Ref 2 and this study and try using different turning angles and splitting the flow into two separate turns. Figure 30 show ideas on what might be attempted with flow choking, flow turning cascades. This type of work should put into practice the techniques of using the water table

for initial flow visualization work and using the gasdynamic tests for quantitative analysis.

Another recommendation is an investigation into the acoustic feedback of back pressure fluctuations to the internal shock dynamics. This project could establish known back pressure variation amounts and then couple these dynamic back pressures to the internal diffuser design to quantify the effects.

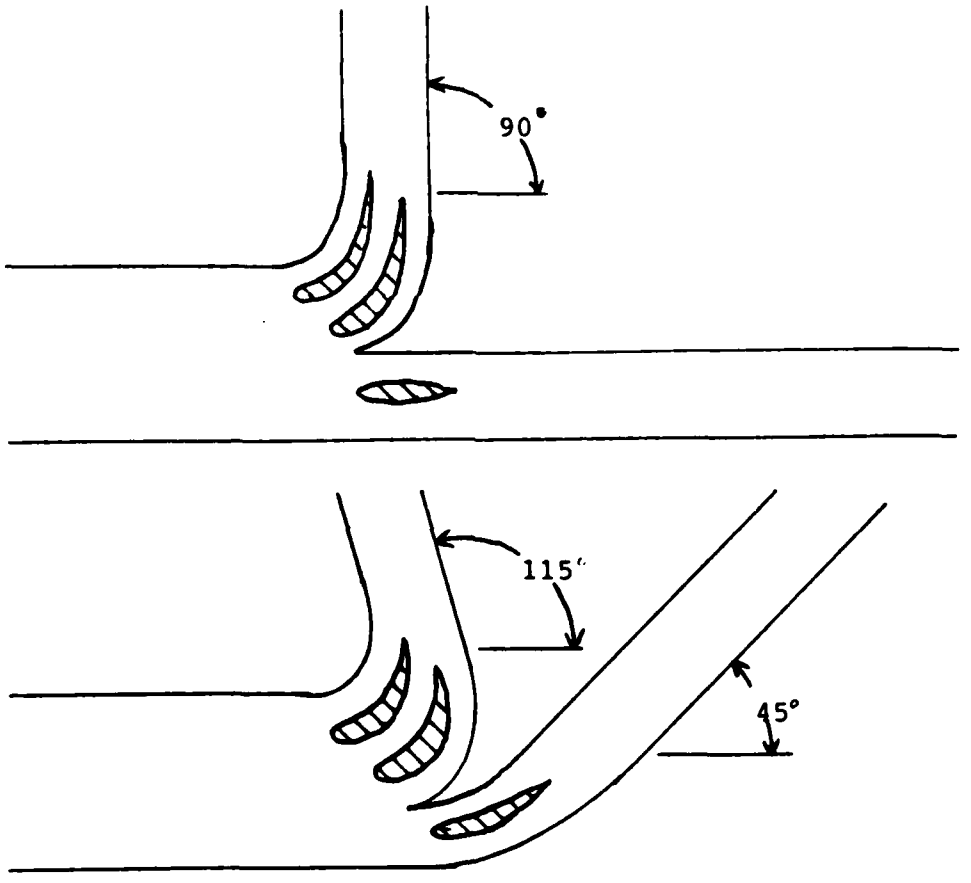

Fig 30 Ideas for Flow Choking, Flow Turning Cascades

BIBLIOGRAPHY

1. Ames Research Staff. Equations, Tables, and Charts For Compressible Flow. NACA Report 1135, 1953.

2. Baird, Jason Design of Choking Cascade Turns. MS Thesis. Wright-Patterson AFB, OHIO: Air Force Institute of Technology, December 1982. (GAE/AA/82D-3).

3. East, L.F. "The Application of a Laser Anemometer to the Investigation of Shock-Wave Boundary-Layer Interaction. AGARD Conference Proceedings No. 193, 1976.

4. Fleming, M.L. and Watson, T.L. Ducted Rocket Inlet Characterization Program. AFRPL-TR-69-99 Part II, Missiles and Space Division, LTV Aerospace Corporation, Dallas Tx, Dec 1968. (AD 501775).

5. Heines, A. Personal Interview. The Marquardt Company, Van Nuys Ca, 17 March 1984.

6. Hill,Phillip G. and Peterson, Carl R. Mechanics and Therodynamics of Propulsion. Reading, Massachusetts: Addison-Wesley Publishing Company, 1970.

7. Huzel, Sieter K. et al. Design of Liquid Propellant Rocket Engines (Second Editon). Washington: National Aeronautics and Space Administration, 1971.

8. Liepmann, H.W. and Roshko, A. Elements of Gasdynamics, New York: John Wiley and Sons, Inc., 1957.

9. Mulenburg, Gerald M. An Experimental Study of the Effect of Inlet Geometry on Flow and Performance of a Supersonic Nozzle. MS Thesis. Wright-Patterson AFB, OHIO: Air Force Institute of Technology, March 1969. (GAM/ME/69-11)

10. Oswatitsch, Klaus Gasdynamics. Translated by Gustav Kuerti. New York: Academic Press Inc., 1956.

11. Prandtl, Ludwig Essentials of Fluid Dynamics. New York: Hafner Publishing Company, 1952.

12. Ramjet Applications Section, Personal Interviews, AFWAL/PORA, Wright-Patterson AFB Oh, 4 Jan through 30 Nov 1984.

13. Shapiro, Asher H. The Dynamics and Thermodynamics of Compressible Fluid Flow. New York: John Wiley and Sons, 1953.

14. Thomas, Arthur N., Jr. Efficient Flow Distribution Control by Means of an Aerodynamic Grid. Van Nuys, California: The Marquardt Company, August 1962.

15. Truley, Richard H., Jr. et al. Supersonic Diffuser with Shock Posistiong Means. Washington: United States Patent Office, Patent Number 2,968,147. Patented 17 January 1961.

16. Turchetti, A.J. and Robertson, J.M. "Design of Vaned-Turns for a Large water Tunnel." Paper Number 48-15. Presented to the Semi-Annual Meeting of the ASME, 30 May - 4 June 1948. New York: American Society of Mechanical Engineers, 1948.

Appendix A: One Dimensional Analysis

Sizing of the internal diffuser throat was accomplished by using equation 1 in Table A-1 and knowledge of the mass flow capabilities of the air supply. A target value of 1.1 lbm/sec at a temperature of 532 R and a total pressure of 30 psia was used. The actual system could give 100 psig at a mass flow around 0.5 lbm/sec, so a lower pressure was used to get the higher mass flows. Equation 1 gave an area of the throat of 1.58 square inches, which was rounded off to 1.6 square inches for this evaluation.

The second throat area was sized to give a theoretical stagnation pressure ratio of 0.8 when both throats were sonic. Having a constant mass flow and assuming the stagnation temperature does not change through the normal shock, equation 1 reduces to : At1 Po1 = At2 Po2. The resulting relationship gave a second throat area of two square inches.

In reference 4, one of the criteria for a well designed aerogrid was to have a Mach number at the second throat between 0.4 and 0.6 when the first throat was just sonic, (critical inlet operation). Using the stream tube relationships (Eqn 2 Table A-1), the mach number for an area ratio of 0.8 was 0.55, which is within the design criteria.

The determination of expansion ratio for the diffuser was acomplished using stream tube relationships. For this study an exit mach number of 0.3 was selected. The exit

area to throat area ratio was calculated to be 2.50.

Theoretical pressure recovery values for the internal diffuser normal shock used equations 2,3 and 4 in Table A-1. First an upstream mach number was derived from equation 2 by knowing the shock position from the schlieren photographs. Then the pressure recovery was computed by appling equation 3 into equation 4.

Table A-1: Compressible Flow Relations

Mass Flow at Throat

$$(1)\quad MF = \frac{A_t P_o \sqrt{k}}{\sqrt{R}\, T_o} \left(\frac{2}{k+1}\right)^{(k+1)/2(k-1)} \qquad \text{(Ref 6: 49)}$$

Stream-Tube Area Relations

$$(2)\quad \frac{A^*}{A} = \frac{216}{125} M \left(1 + \frac{M^2}{5}\right)^{-3} \qquad \text{(Ref 1: Eqn 80)}$$

Normal Shock Relations

$$(3)\quad \frac{P_2}{P} = Z = 7\frac{M_1^2}{6} - 1 \qquad \text{(Ref 1; Eqn 93)}$$

$$(4)\quad PR = \frac{P_{t2}}{P_{t1}} = \left(\frac{1}{Z}\right)^{2.5} \left(\frac{6\ Z+1}{Z+6}\right)^{3.5} \qquad \text{(Ref 1: Eqn 111)}$$

Appendix B: Pressure Profiles

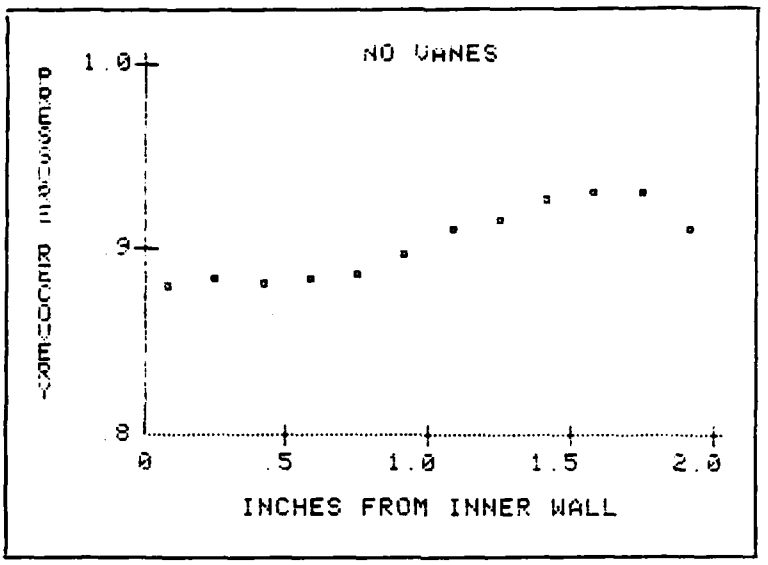

B-1 Unvaned Turn, Critical Operation, 1.076 lbm/sec

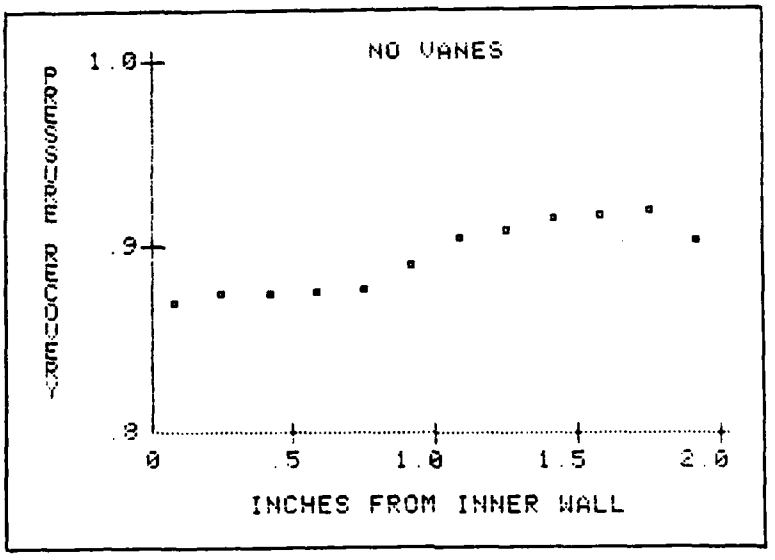

B-2 Unvaned Turn, Critical Operation, 1.185 lbm/sec

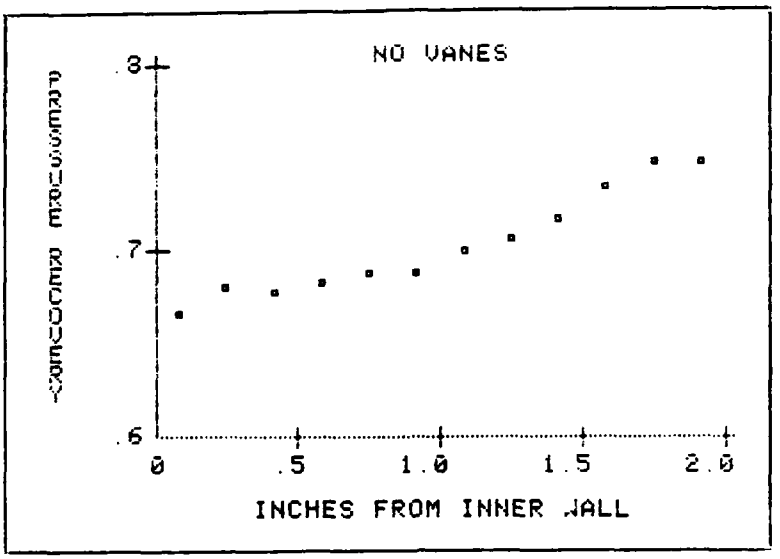

B-3 Unvaned Turn, Intermediate Back Pressure

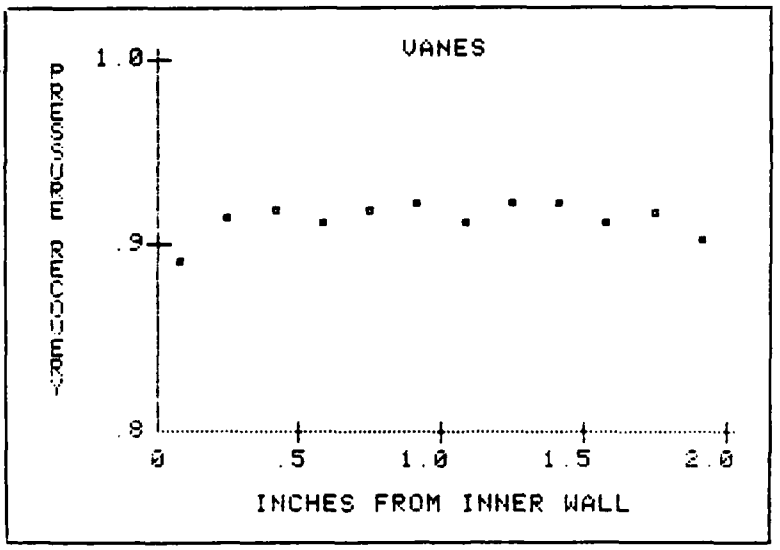

B-4 Vaned Turn, Critical Operation, 1.078 lbm/sec

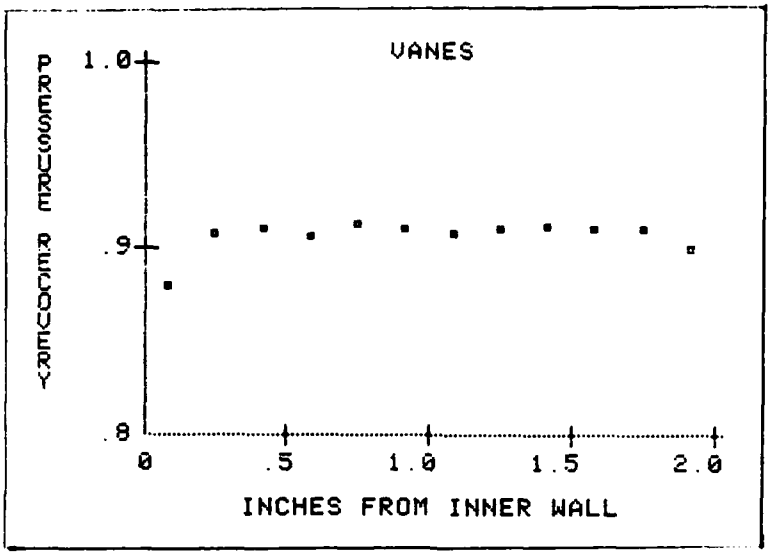

B-5 Vaned Turn, Critical Operation, 1.179 lbm/sec

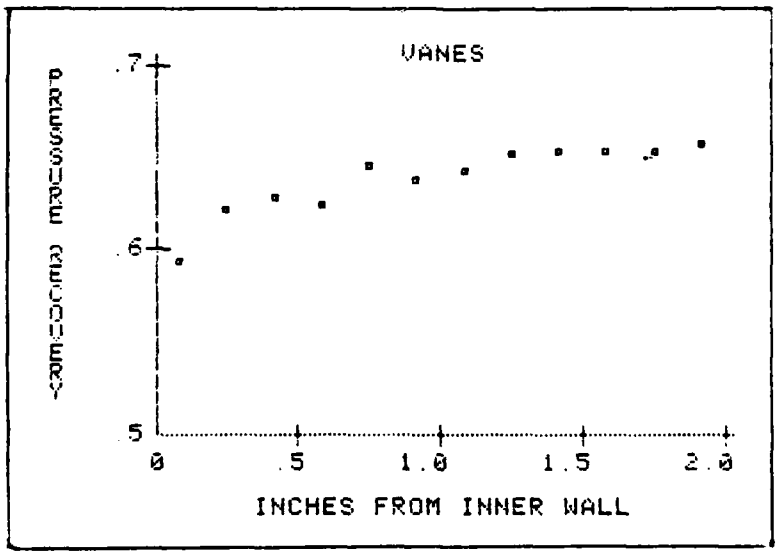

B-6 Vaned Turn, Minimum Back Pressure

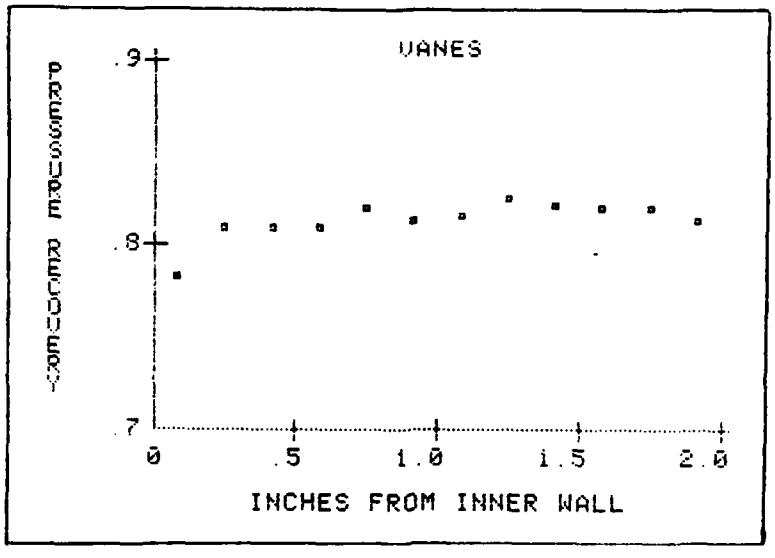

B-7 Vaned Turn, Intermediate Back Pressure

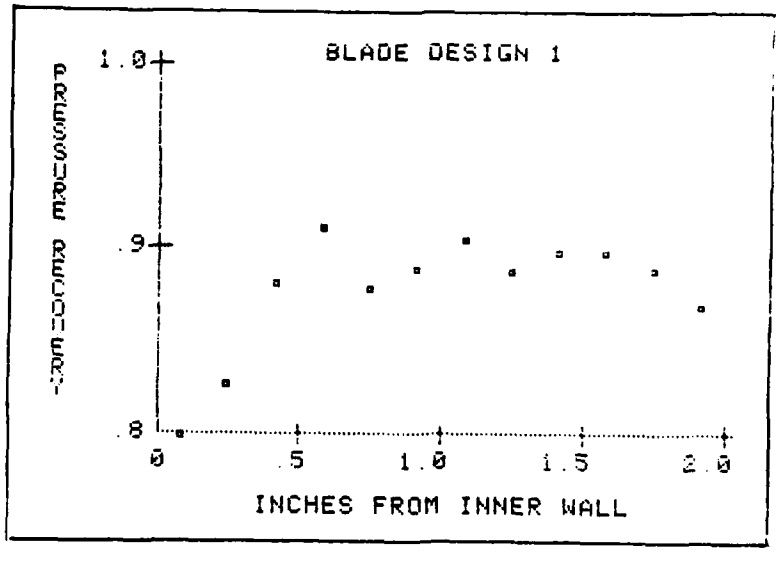

B-8 Blade 1, Critical Operation

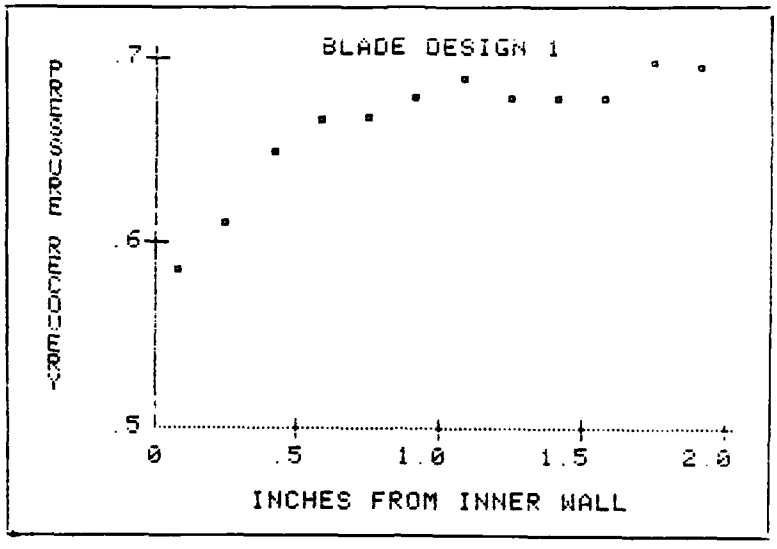

B-9 Blade 1, Minimum Back Pressure

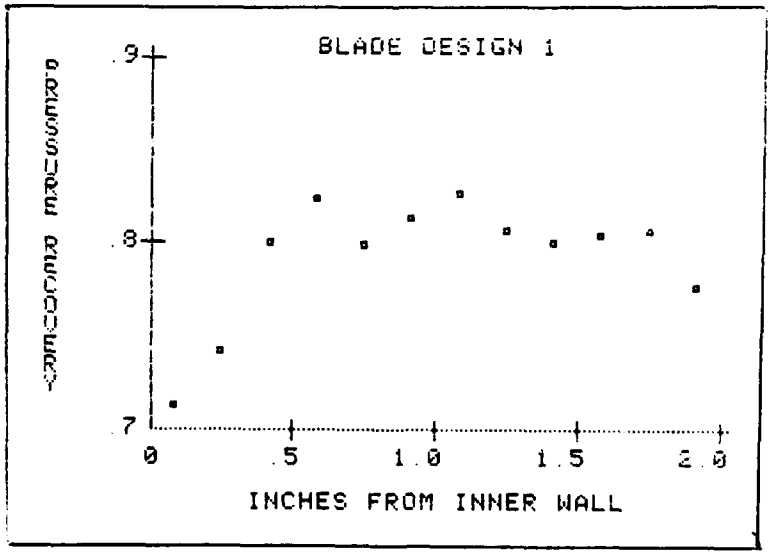

B-10 Blade 1, Intermediate Back Pressure

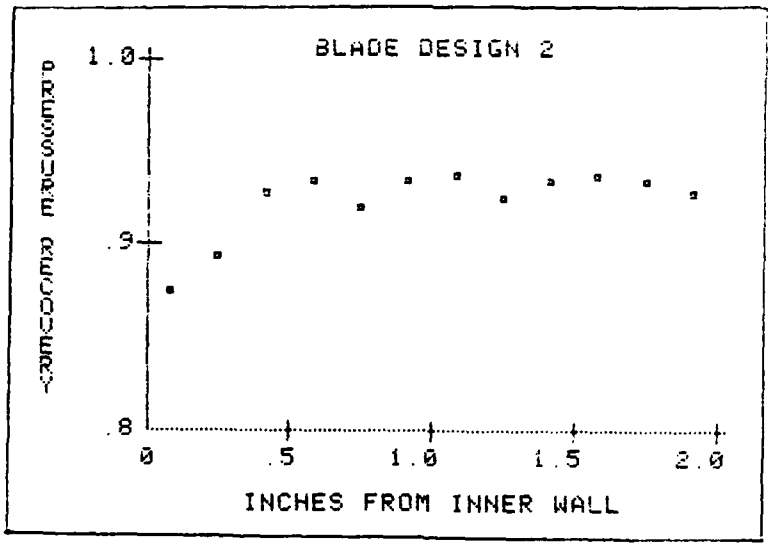

B-11 Blade 2, Critical Operation, .6193 lbm/sec

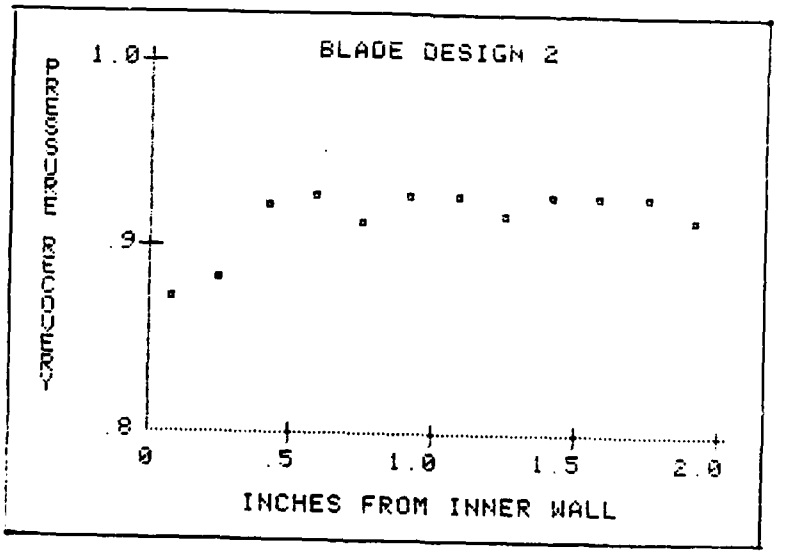

B-12 Blade 2, Critical Operation, .7204 lbm/sec

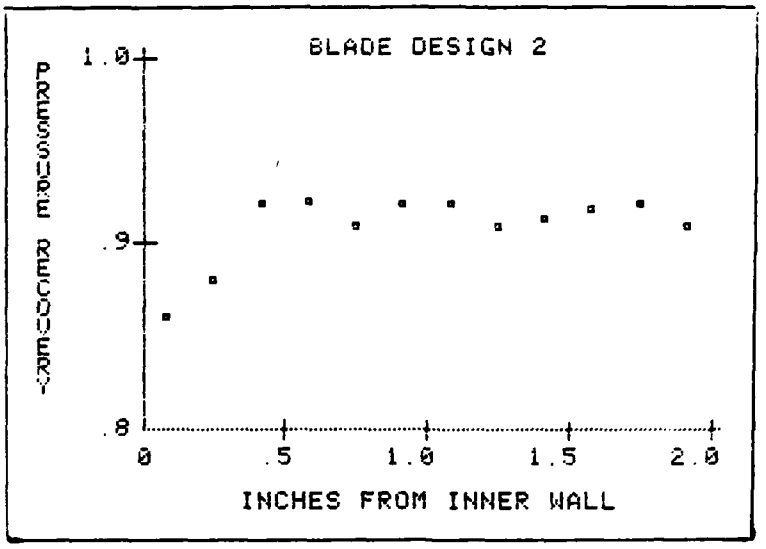

B-13 Blade 2, Critical Operation, .8911 lbm/sec

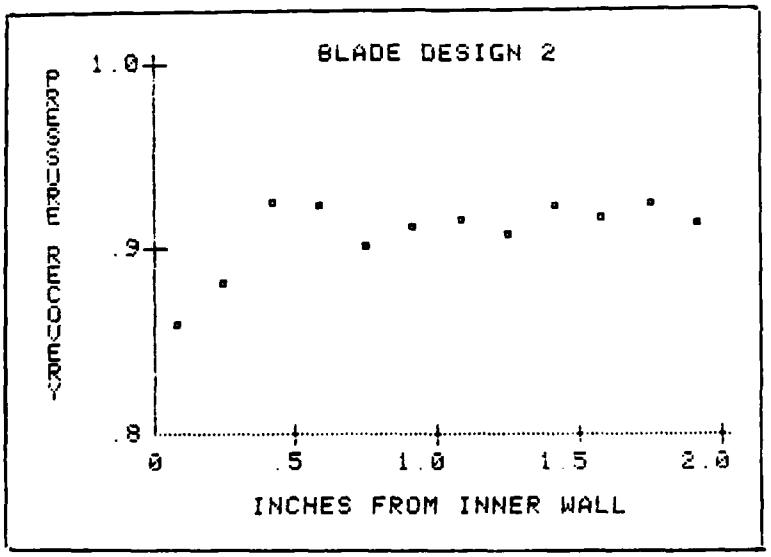

B-14 Blade 2, Critical Operation, .9674 lbm/sec

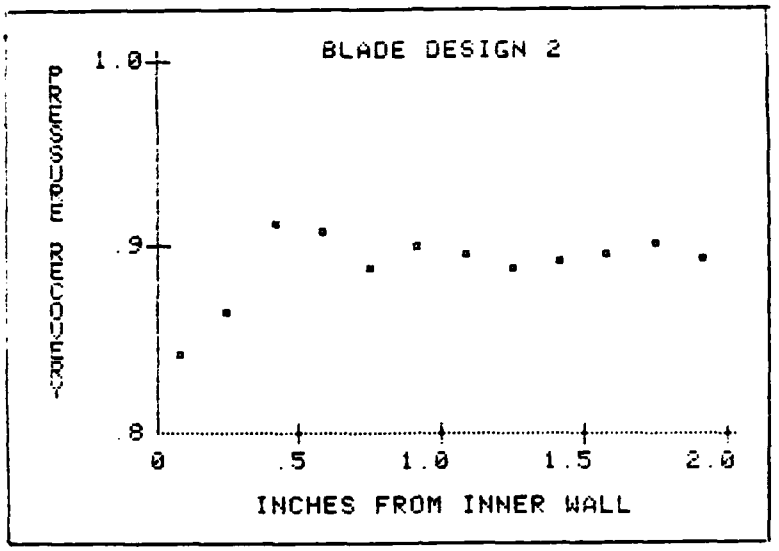

B-15 Blade 2, Critical Operation, 1.069 lbm/sec

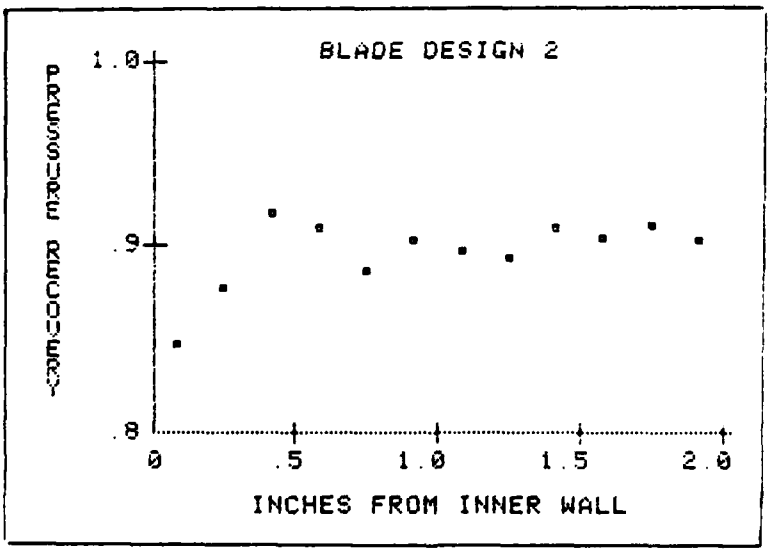

B-16 Blade 2, Critical Operation, 1.076 lbm/sec

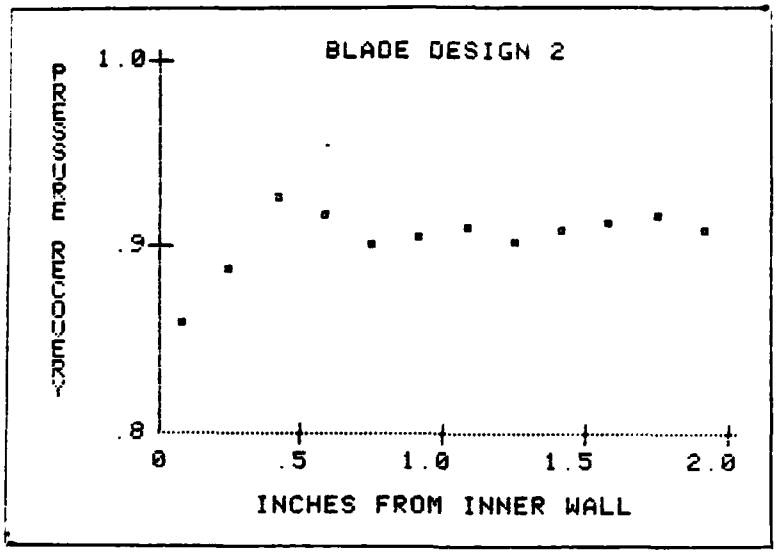

B-17 Blade 2, Critical Operation, 1.079 lbm/sec

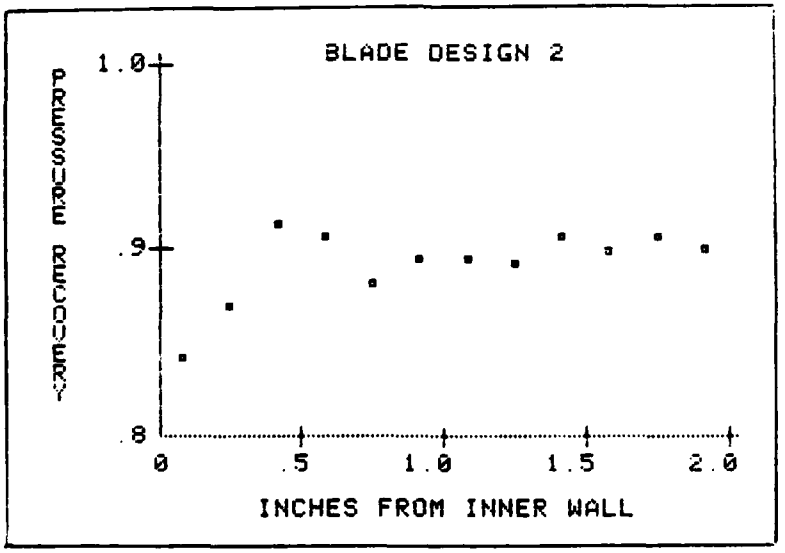

B-18 Blade 2, Critical Operation, 1.185 lbm/sec

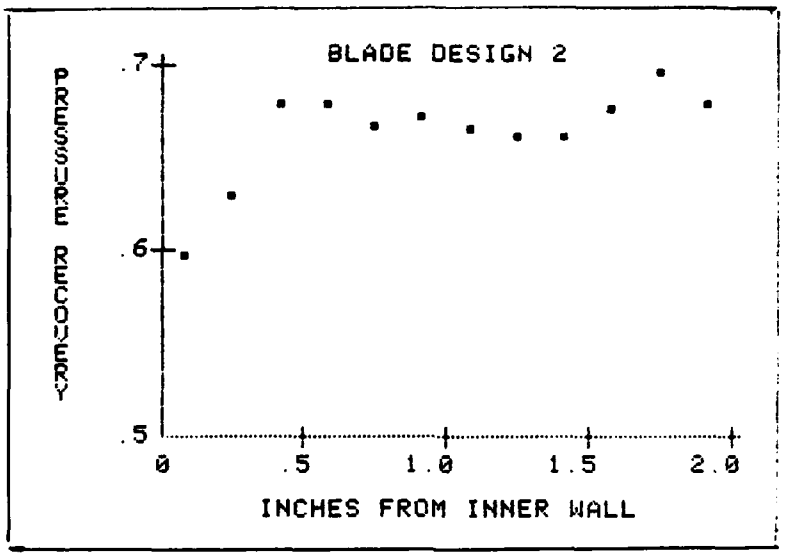

B-19 Blade 2, Minimun Back Pressure

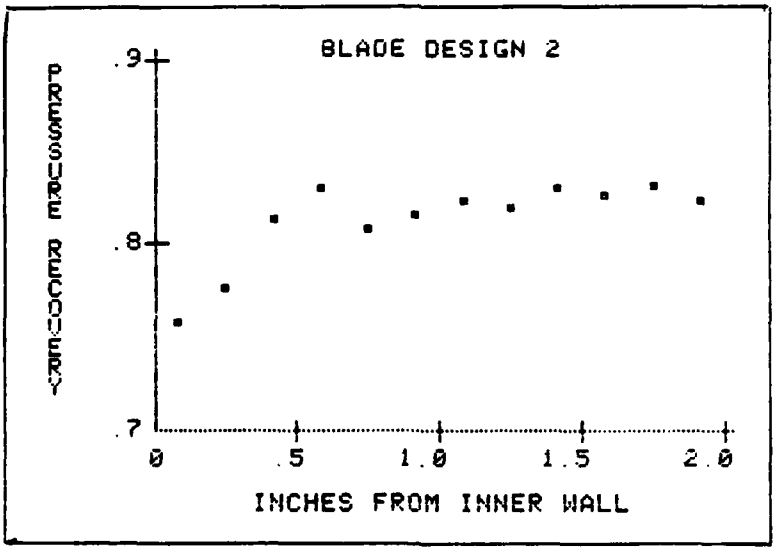

B-20 Blade 2, Intermediate Back Pressure

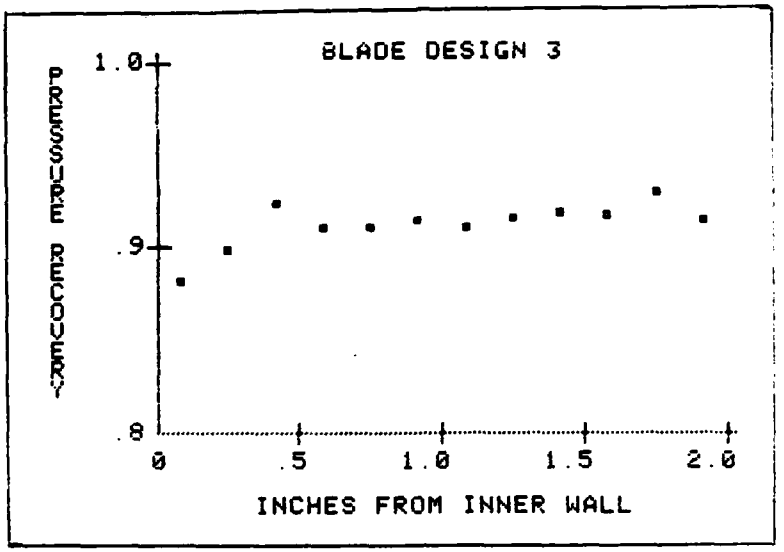

B-21 Blade 3, Critical Operation, 1.076 lbm/sec

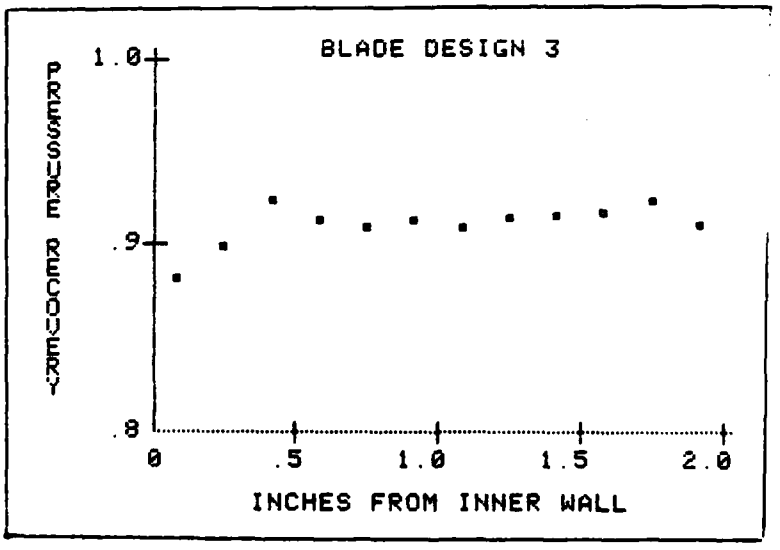

B-22 Blade 3, Critical Operation, 1.185 lbm/sec

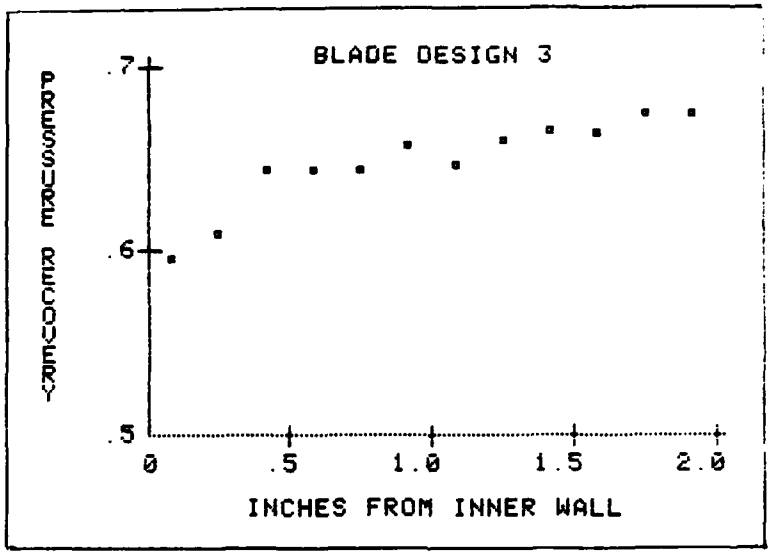

B-23 Blade 3, Minimum Back Pressure

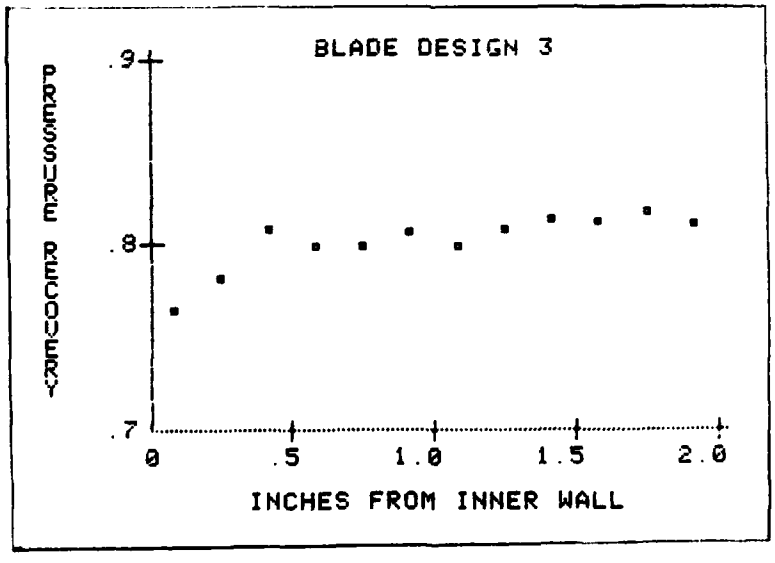

B-24 Blade 3, Intermediate Back Pressure

VITA

Dennis R Perez [redacted] He [redacted] enlisted in the United States Air Force. After four years working in the precision measuring equipment career field, he was selected to attend the University of Texas at Austin, under the Airmen Education and Commissioning program, for which he recieved the degree of Bachelor of Science in Aerospace Engineering in December 1979. In April 1980 he recieved his commission from the Officer Training School at Lackland AFB, Texas. He then served as a Strategic Air Launched Missile Propulsion Project Officer at the Air Force Rocket Propulsion Laboratory at Edwards AFB, California, until entering the School of Engineering, Air Force Institute of Technology, in June 1983.

[redacted]

UNCLASSIFIED

SECURITY CLASSIFICATION OF THIS PAGE

REPORT DOCUMENTATION PAGE

1a. REPORT SECURITY CLASSIFICATION UNCLASSIFIED	1b. RESTRICTIVE MARKINGS
2a. SECURITY CLASSIFICATION AUTHORITY	3. DISTRIBUTION/AVAILABILITY OF REPORT Approved for public release; distribution unlimited.
2b. DECLASSIFICATION/DOWNGRADING SCHEDULE	
4. PERFORMING ORGANIZATION REPORT NUMBER(S) AFIT/GAE/AA/84D-21	5. MONITORING ORGANIZATION REPORT NUMBER(S)
6a. NAME OF PERFORMING ORGANIZATION School of Engineering 6b. OFFICE SYMBOL (If applicable) AFIT/AA	7a. NAME OF MONITORING ORGANIZATION
6c. ADDRESS (City, State and ZIP Code) Air Force Institute of Technology Wright-Patterson AFB, Ohio 45433	7b. ADDRESS (City, State and ZIP Code)
8a. NAME OF FUNDING/SPONSORING ORGANIZATION 8b. OFFICE SYMBOL (If applicable)	9. PROCUREMENT INSTRUMENT IDENTIFICATION NUMBER
8c. ADDRESS (City, State and ZIP Code)	10. SOURCE OF FUNDING NOS. PROGRAM ELEMENT NO. / PROJECT NO. / TASK NO. / WORK UNIT NO.
11. TITLE (Include Security Classification) See Box 19	
12. PERSONAL AUTHOR(S) Dennis R. Perez, B.S., Capt, USAF	
13a. TYPE OF REPORT MS Thesis 13b. TIME COVERED FROM _____ TO _____	14. DATE OF REPORT (Yr., Mo., Day) 1984 December 15. PAGE COUNT 78
16. SUPPLEMENTARY NOTATION	

17. COSATI CODES			18. SUBJECT TERMS (Continue on reverse if necessary and identify by block number)
FIELD	GROUP	SUB. GR.	Cascades, Diffusers, Inlets, Intakes
20	04		
21	05		

19. ABSTRACT (Continue on reverse if necessary and identify by block number)

Title: GASDYNAMIC EVALUATION OF CHOKING CASCADE TURNS

Thesis Chairman: Dr William C. Elrod

Approved for public release: IAW AFR 190-17.

LYNN E. WOLAVER 25 Feb 85
Dean for Research and Professional Development
Air Force Institute of Technology (AU)
Wright-Patterson AFB OH 45433

20. DISTRIBUTION/AVAILABILITY OF ABSTRACT UNCLASSIFIED/UNLIMITED ☒ SAME AS RPT. ☐ DTIC USERS ☐	21. ABSTRACT SECURITY CLASSIFICATION UNCLASSIFIED
22a. NAME OF RESPONSIBLE INDIVIDUAL Dr William C. Elrod	22b. TELEPHONE NUMBER (Include Area Code) 513-255-3517 22c. OFFICE SYMBOL AFIT/EN

DD FORM 1473, 83 APR EDITION OF 1 JAN 73 IS OBSOLETE.

UNCLASSIFIED

SECURITY CLASSIFICATION OF THIS PAGE

Uses for ram air in airborn vechiles are increasing along with the need for sophisticated ducting of the compressed air. Inlets operating supercritically, a normal shock in the subsonic diffuser, use an aerodynamic grid to control the normal shock posistion to a region of low total pressure losses. Turning of the flow requires long radius curves to maintain the total pressure. This study combines the internal shock posistioning and flow turning into a flow choking cascade turn with a short radius. Several sets of 90 degree turning sections, for turning compressed air, were selected, designed, and tested gas dynamically. Two of the turn sections were totally subsonic and only turned the air flow. Two other sections turned and choked the flow during supercritical inlet operation. These flow controllers perform the same function as an aerodynamic grid and flow turning vanes used in current internal compressible airflow designs . These tests correlated the suitability of using a water table versus a gasdynamic apparatus for determining the flow control capabilities and pressure recovery of the cascades. The subsonic only turning section gave the best pressure recovery and total pressure distribution along the turning axis, but allowed the supercritical internal shock to move towards large shock/boundary layer interaction. The two shock positioning cascades provided good internal shock control with only slightly lower pressure recovery. Further investigation is needed of the effects of back pressure fluctuations on the flow dynamics.